Soils Quality Assessment in Kambele Gold Mining Area using Multivariate Statistical Analysis Approach

SOP TAMO Berthelot[1*]; MEFOMDJO FOTIE Blanche[2]; OTIA KAKWOUN Yvette[1]; TARKWA Jean Baptiste[1]; TCHUIKOUA Louis Bernard[2]; MAMBOU NGUEYEP Luc Leroy[1,3]

[1]School of Geology and Mining Engineering, University of Ngaoundéré, P.O. Box 115, Meiganga, Cameroon.

[2]Department of Geography, Faculty of arts, letter and social science, University of Yaoundé 1, Cameroon.

[3]Laboratory of Mechanics and Materials of Civil Engineering (L2MGC), CY Cergy Paris University, 5 Mail Gay Lussac, Neuville sur Oise, F-95031 Cergy-Pontoise Cedex, France.

DOI: https://doi.org/10.51244/IJRSI.2026.1306000175

Received : 13 April 2026 ; Accepted : 18 April 2026 ; Published : 29 June 2026

ABSTRACT

This study assesses soil quality in the Kambele gold mining area (Eastern Cameroon) through integrated physico-chemical characterization, pollution index calculation, multivariate statistical analysis, and spatial mapping. Thirty surface soil samples (0-5 cm depth) were collected in June 2021 using systematic random sampling across the 30 km² study area. Physico-chemical parameters (pH, electrical conductivity, organic matter, moisture content) and heavy metal concentrations (Cr, Ni, Cu, Zn, Pb, Fe, Mn, As) were determined using XRF spectrometry (Skyray EDX POCKET III). Results reveal acidic soils (pH 5.12-6.22) with elevated electrical conductivity (96-416 µS/cm) and variable organic matter (0.30-1.42%). Heavy metal concentrations show significant contamination exceeding WHO guidelines for Pb (max 114 ppm), Cu (485 ppm), Ni (655 ppm), As (60 ppm), and Fe (121,611 ppm). Comprehensive pollution assessment using 15 indices (EF, Igeo, CF, PI, PLI, PIVector, MEC, CSI, Cdeg, Nemerow, Potential Ecological Risk, ExF, mCd) indicates moderate to extreme contamination, with Cu and Ni showing the highest enrichment. Principal Component Analysis (PCA) explains 72.83% of total variance, identifying three contamination sources : natural pedogeochemical background (PC1 : 49.93%), mining-related inputs (PC2: 22.90%), and mixed anthropogenic sources (PC3: 12.07%). Spatial kriging maps reveal heterogeneous contamination patterns with identified hotspots at Djengou washing station (E28) and site E8. Human health risk assessment indicates non-carcinogenic hazard indices exceeding USEPA thresholds for children (HI > 1) at multiple locations, primarily driven by As, Pb, and Cu exposure. These findings underscore the urgent need for targeted remediation strategies, including phytoremediation for moderately contaminated areas, soil amendments for pH adjustment, and containment measures for severe hotspots. This study provides the first comprehensive environmental baseline for Kambele, supporting evidence-based policy interventions and community health protection measures.

Keywords : Mining exploitation, soils, contamination, pollution, heavy metals, health risk assessment, spatial analysis

INTRODUCTION

Industrial activities such as mining are among the most environmentally polluting. With increasing artisanal and semi-mechanized exploitations, environmental components are significantly impacted. The expansion of industrial activities, particularly mining and smelting, has resulted in a broad range of environmental problems (Lee et al., 2019). Soils become contaminated through the accumulation of toxic heavy metals and metalloids (Csavina et al., 2012). These contaminants, emitted from mining and ore processing industries, are considered hazardous waste, causing local and diffuse soil pollution (Kim et al., 2022). Generally, soils at industrial sites

ISSN No. 2321-2705 | DOI: 10.51244/IJRSI |Volume XIII Issue VI June 2026

and in natural environments are exposed to distinct groups of toxic heavy metal contaminants (Pawan, 2012 ; Caeiro et al., 2015 ; Mandeng et al., 2019).

To prevent soil heavy metal contamination from industrial and mining activities, researchers have investigated heavy metal contamination in various regions. Zhou et al. (2007) studied soil contamination near the Dabaoshan Mine, China, finding that Cu, Zn, Cd, and Pb contamination has persisted for decades. Teixeira et al. (2018) reported high total and available contents of Cu, Mo, Pb, and Zn in the Serra Pelada gold mining area (Brazil), posing risks to both ecosystems and local populations. Getaneh et al. (2006) found elevated Ni, Cr, Cu, V, Zn, Pb, and As concentrations in primary gold sites in Southern Ethiopia. Matini et al. (2011) reported heavy metal concentrations above European Union standards in soils from an abandoned lead ore treatment plant in Congo Brazzaville. In Namibia, Marta et al. (2014) found arable soils with high Cu and Pb concentrations indicating severe contamination. Gyamfi et al. (2019) reported extreme soil pollution with Fe, Pb, Zn, As, Mn, and Cu in Kokotesua, Ghana. Ourou et al. (2019) found unacceptably high Zn and Pb concentrations in soils from the abandoned Edendale mine, South Africa.

In Cameroon, several studies have documented mining-related contamination. Léopold et al. (2016) found As, Cr, Cd, Cu, Pb, and Sb levels above Upper Continental Crust averages in Meiganga. Mominou et al. (2018) characterized six gold mining sites in Bétaré-Oya, finding arsenic, nickel, and lead contamination in 12 of 22 samples. Dallou et al. (2018) studied environmental pollution by heavy metals in Batouri and Betare-Oya, reporting polluted soils. Mambou et al. (2020) observed high Cu, Ni, Mn, Fe, and Cr concentrations in sediments from Betare-Oya. Ayiwouo et al. (2022) assessed trace metal contamination in sediments along the Lom River, showing moderate to significant contamination with Ni and Cu exceeding average shale concentrations.

Soil heavy metals can transfer to food and ultimately to consumers through bioaccumulation (Affum et al., 2020 ; Adenuga et al., 2022 ; Awasthi et al., 2022 ; Mmaduakor et al., 2022). Several metals and metalloids are classified as human carcinogens by the U.S. Environmental Protection Agency and the International Agency for Research on Cancer (IARC) (Tchounwou et al., 2012). The Institute for Health Metrics and Evaluation attributes more than half a million deaths annually to lead exposure (Sawant et al., 2017). Cadmium is classified as a category 1 human carcinogen, associated with lung, prostate, pancreas, and kidney cancers (Tokar et al., 2010 ; IARC Monographs, 2012). Inorganic arsenic compounds are Group 1 carcinogens, linked to skin, bladder, lung, kidney, and liver cancers (Rossman, 2003).

A field survey in Kambele revealed that populations are primarily affected by waterborne and skin diseases, with evidence of early mortality (Mokam et al., 2013 ; Funoh, 2014). This study investigates, for the first time, the relationship between health conditions in Kambele and artisanal/semi-mechanized gold mining activities through comprehensive environmental soil assessment. The findings will support the development of an environmental management plan to minimize health risks associated with gold mining in this locality.

MATERIALS AND METHODS

Study Area

Location

The Batouri area is located in the Eastern region of Cameroon (04°21' to 04°29' North and 14°17' to 14°29' East), within a humid tropical climatic zone. It comprises the localities of Djengo, Mongonam, Bote, Metalicon, and Kambele. The study area lies within the so-called "Eastern gold district," the most mineralized area in Cameroon (Tchouankam et al., 2020). Figure 1 shows the location of the Kambele mining zone.

Climate

The region experiences a warm and wet equatorial climate with two rainy seasons separated by two dry seasons : mild rainy period (mid-March to June), mild dry period (June to mid-August), heavy rainy season (mid-August to mid-November), and pronounced dry season (mid-November to mid-March). Average annual precipitation ranges between 1500-2000 mm, with mean temperatures around 23°C (PCD, 2019).

Geomorphology and Hydrography

The relief is relatively flat with average altitudes between 600-1000 m, featuring undulating landscapes with forest and savannah zones (PCD, 2019) (Figure 2). The hydrographic network comprises several rivers (Kpwangala, Antobi, Tekam, Djengou, Amorcelin, Mboscorow, Mbil) converging into the Kadey River, displaying a dendritic drainage pattern (Figure 3).

Geology and Petrography

Kambele is situated in the Adamawa-Yade domain of the Pan-African Gold Belt in Cameroon (Poidevin, 1983 ; Nzenti et al., 1988). The geological evolution results from convergence and collision of the São Francisco-Congo Craton, West African Craton, and a Pan-African Mobile Belt (Castaing et al., 1994). The area is underlain by granitic rocks including alkali-feldspar granite, syeno-monzogranite, granodiorite, and tonalite. The Pan-African belt in Cameroon is characterized by continent-continent collision and post-collision processes (Toteu et al., 2004). Figure 4 displays the main rock types.

Soils and Vegetation

Two principal soil types occur : ferralitic and hydromorphic soils. Hydromorphic soils develop in conditions of excess moisture, found primarily in swampy areas and along river courses (PCD, 2019). Parent material consists mainly of quartzite and granites. Vegetation comprises herbaceous savannah in the north and luxuriant forest in the south, though bushfires, deforestation, and mining activities have significantly degraded vegetation cover.

SAMPLING DESIGN AND COLLECTION

Sampling Strategy and Rationale

A systematic random sampling approach was adopted to account for the irregular morphology of the study area. Thirty (30) sampling points were strategically distributed across the Kambele mining zone to ensure representative coverage of different land use types, mining intensity gradients, and environmental compartments. Sample locations were selected using a grid-based approach with 1 km spacing, adjusted to access constraints and mining activity distribution. The selection considered : (a) active mining areas with ongoing extraction ; (b) abandoned mining sites at various stages of rehabilitation ; (c) processing areas (washing stations) ; (d) waste disposal zones ; (e) reference areas with minimal mining disturbance ; and (f) agricultural fields potentially impacted by mining activities.

Justification for n=30: This sample size was determined based on: (i) the spatial heterogeneity of the 30 km² study area; (ii) statistical power considerations for multivariate analysis (minimum 5-10 samples per variable ratio; 8 metals × 5 = 40, reduced to 30 due to field constraints); (iii) comparability with similar studies (Dallou et al., 2018 used 22 samples; Mominou et al., 2018 used 20 samples); (iv) logistical constraints associated with field access in the rainy season; and (v) cost-effectiveness considerations for laboratory analyses.

Field Collection Protocol

Sample collection was conducted on June 30, 2021, during the mild rainy season, following standardized protocols (Carter & Gregorich, 2008). At each predetermined position, surface vegetation and debris were carefully removed by hand, and the area was leveled. Soil samples (approximately 1 kg each) were collected from the surface horizon at 0-5 cm depth using a stainless steel trowel to avoid metal contamination. The top 2-3 mm of soil was first removed to eliminate atmospheric deposition artifacts, and samples were taken from the center of the cleared area.

This depth was selected because : (i) the study area lacks well-developed soil profiles due to recent mining disturbance ; (ii) surface soils are most relevant for assessing anthropogenic contamination ; (iii) this depth captures the zone of maximum metal accumulation from atmospheric deposition and mining activities ; and (iv) it allows comparison with similar studies (Mominou et al., 2018 ; Dallou et al., 2018).

ISSN No. 2321-2705 | DOI: 10.51244/IJRSI |Volume XIII Issue VI June 2026

Sample Handling and Transport

Each sample was immediately sealed in labeled polyethylene bags (pre-washed with 10% HNO_3 and rinsed with deionized water), placed in opaque containers to prevent photodegradation, and transported to the laboratory in cooled insulated boxes (4°C) within 24 hours of collection. GPS coordinates were recorded using a GARMIN eTrex 10 receiver (accuracy ±3 m) for all sampling points (Table 1).

SAMPLE PREPARATION AND PRE-TREATMENT

Drying and Sieving

Samples were air-dried at ambient temperature (25-28°C) for 72 hours in a clean, dust-free laboratory environment to prevent contamination. Drying was conducted in paper-lined trays, and samples were periodically turned to ensure uniform drying. After drying, samples were gently crushed using an agate mortar and pestle to disaggregate soil aggregates, then sieved through a 2-mm nylon mesh (ASTM standard No. 10) to remove gravel, roots, and organic debris. Approximately 50 g of <2 mm fraction was then ground to <75 µm (ASTM No. 200) using an agate planetary ball mill (Fritsch Pulverisette 5) for 10 minutes at 300 rpm to achieve particle size suitable for XRF analysis. The <2 mm fraction was retained for physico-chemical analyses.

Sub-sampling and Homogenization

Sub-samples were obtained using a riffle splitter (Jones-type) to ensure representative sampling for different analyses. For each sample, three aliquots were prepared :

- Aliquot 1 : 5 g for XRF analysis (ground to <75 µm)
- Aliquot 2 : 10 g for physico-chemical parameters (pH, EC, OM, MC)
- Aliquot 3 : Archive sample (50 g) stored in sealed polyethylene bags at 4°C

ANALYTICAL METHODS

X-Ray Fluorescence Spectrometry (XRF)

Instrumentation : Elemental concentrations were determined using a Skyray EDX POCKET III energy-dispersive X-ray fluorescence spectrometer (Skyray Instruments Inc., USA), equipped with a rhodium (Rh) anode X-ray tube (50 kV, 1 mA) and a silicon drift detector (SDD) with 125 eV resolution at Mn Kα.

Analytical Conditions : All analyses were performed under the following conditions : helium atmosphere, measurement time of 300 seconds per sample (divided into 120 seconds for light elements and 180 seconds for heavy elements), voltage settings of 15 kV (for light elements) and 45 kV (for heavy elements), current of 80 µA, and analysis area of 10 mm^2. Three replicates were measured per sample, and results were averaged.

Calibration and Quality Control : Instrument calibration was performed daily using standard reference materials (NIST SRM 2710a Montana Soil and SRM 2709 San Joaquin Soil). Matrix correction was applied using the fundamental parameters (FP) method with Compton/Rayleigh scattering ratio normalization. Additionally, a standard addition approach was used for selected samples to verify matrix effects. Elemental concentrations were quantified using the EDX Pocket III software (version 2.3), applying the following settings : (a) background subtraction using the SNIP algorithm ; (b) peak deconvolution using the Gaussian fitting model ; (c) inter-element correction using the Lachance-Traill algorithm.

Detection Limits and Precision : Detection limits (3σ criterion) were : Cr (3 mg/kg), Ni (4 mg/kg), Cu (3 mg/kg), Zn (2 mg/kg), Pb (5 mg/kg), As (2 mg/kg), Mn (4 mg/kg), Fe (50 mg/kg). Analytical precision, assessed as relative standard deviation (RSD) of duplicate analyses, was <5% for all elements at concentrations >10× detection limit, and <10% for concentrations near detection limits.

ISSN No. 2321-2705 | DOI: 10.51244/IJRSI |Volume XIII Issue VI June 2026

pH Measurement

Soil pH was determined in a 1 :2.5 (w/v) soil-to-deionized water suspension using a HACH HQ40d pH meter (Hach Company, USA) equipped with a combination glass electrode (intelliCAL PHC101). Before measurement, the pH meter was calibrated using standard buffer solutions (pH 4.01, 7.00, and 10.01) at 25°C. Soil suspensions were shaken for 10 minutes, allowed to equilibrate for 60 minutes, and pH was recorded after stabilization (drift <0.01 units/min). All measurements were performed in triplicate.

Electrical Conductivity

Electrical conductivity (EC) was measured in the same 1 :2.5 soil : water suspension using a HACH HQ40d EC meter (Hach Company, USA) with a conductivity cell (intelliCAL CDC401) at 25°C. The meter was calibrated using 1413 µS/cm and 12,880 µS/cm KCl standard solutions. EC values were corrected to 25°C using the temperature coefficient.

Organic Matter Determination

Soil organic matter (OM) was determined by the Walkley-Black wet oxidation method (Walkley, 1947). The procedure involved : (1) 0.5 g air-dried soil (<2 mm) placed in a 250 mL Erlenmeyer flask ; (2) 10 mL of 0.167 M $K_2Cr_2O_7$ (potassium dichromate) added, followed by 20 mL of concentrated H_2SO_4 ; (3) mixture allowed to react for 30 minutes ; (4) 100 mL deionized water added ; (5) titration with 0.5 M ferrous ammonium sulfate (FAS) using 1 mL of diphenylamine indicator (1% in H_2SO_4) until the color changed from violet-blue to green ; (6) blank determination without soil. OM content was calculated using equation (1) :

$$\mathrm{OM}(\%) = \frac{(V_{blank} - V_{sample}) \times M_{FAS} \times 0.3 \times 1.724}{W_{sample}} \times 100 \qquad (1)$$

Where : V_{blank} is the FAS volume for blank (mL), V_{sample} the FAS volume for sample (mL), M_{FAS} the molarity of FAS solution (0.5 M), Wsample the weight of soil (g), 0.3 is the correction factor for incomplete oxidation and 1.724 the conversion factor to convert organic carbon to organic matter.

Moisture Content

Moisture content (MC) was determined by oven-drying method. Approximately 10 g of field-moist soil was weighed in pre-dried (105°C) aluminum tins (W_1). The samples were oven-dried at 105°C for 24 hours until constant weight. After drying, the tins were cooled in a desiccator and reweighed (W_3). MC was calculated using equation (2) :

$$\mathrm{MC}\% = {}^{W_2 - W_3}/_{W_3 - W_1} * 100 \qquad (2)$$

Where : W_1 is the weight of tin (g), W_2 the weight of moist soil + tin (g) and W_3 the weight of dried soil + tin (g).

Quality Assurance and Quality Control (QA/QC)

Comprehensive QA/QC measures were implemented to ensure data reliability :

Field QA/QC

- **Field blanks :** Three field blank samples (sterile quartz sand) were exposed to ambient conditions during sampling to assess airborne contamination. Results showed negligible contamination (<2% of lowest sample concentrations).

ISSN No. 2321-2705 | DOI: 10.51244/IJRSI |Volume XIII Issue VI June 2026

- **Field duplicates :** Three duplicate samples were collected at random locations (E5, E15, E25) to assess field variability. Relative percent differences (RPD) for duplicate pairs ranged from 3.2% (Cu) to 8.7% (Pb), within acceptable limits (<15%).

- **Trip blanks :** One trip blank was carried with samples to assess contamination during transport. No contamination was detected.

Laboratory QA/QC

- **Certified Reference Materials (CRMs) :** NIST SRM 2710a (Montana Soil, highly contaminated) and SRM 2709 (San Joaquin Soil) were analyzed with each batch of 10 samples. Recoveries ranged from 92.3% (Cr) to 107.1% (Ni) (Table S1).

- **Analytical duplicates :** Every 10th sample (n=3) was analyzed in duplicate. Average RSD values were : Cr 4.2%, Ni 3.8%, Cu 3.1%, Zn 4.5%, Pb 5.2%, As 6.3%, Mn 3.9%, Fe 2.8%.

- **Spike recoveries :** Matrix spikes were performed on three samples (E8, E18, E28) by adding 50% of the predicted concentration of selected metals. Recoveries ranged from 85.2% (As) to 112.4% (Pb), acceptable for soil XRF analysis (80-120% range).

- **Reagent blanks :** All chemical reagents were pre-screened for metal contamination. Blank readings were below detection limits for all metals.

- **Instrument stability :** Internal standards (Cu, Zn, and Y) were analyzed every 10 samples to monitor instrument drift. Drift was <2% for all analyses. Recalibration was performed daily and after every 20 samples.

Pollution Indices

Fifteen pollution indices were calculated to provide comprehensive contamination assessment. Background values (GB) for heavy metals were based on average upper continental crust values (Taylor & McLennan, 1985).

Enrichment Factor (EF)

The enrichment factor normalizes metal concentrations to a conservative reference element (Fe) to differentiate anthropogenic from natural sources (equation 3) :

$$EF = \left(C_n/C_{ref}\right)_{Sample} \Big/ \left(B_n/B_{ref}\right)_{background} \quad (3)$$

Where C_n is the concentration of examined element ; C_{ref} the concentration of reference element (Fe) ; B_n the background concentration ; B_{ref} the background concentration of reference element (Fe = 47,200 ppm ; Taylor & McLennan, 1985). EF classifications : <2 minimal enrichment ; 2-5 moderate ; 5-20 significant ; 20-40 very high ; >40 extremely high.

Geo-accumulation Index (Igeo)

Igeo compares current concentrations with preindustrial background levels (equation 4) :

$$I_{geo} = \log 2 \left[C_n / 1.5B_n \right] \quad (4)$$

Where C_n is the measured concentration ; B_n the background value. Igeo classes : 0-1 unpolluted to moderately polluted ; 1-2 moderately polluted ; 2-3 moderately to strongly polluted ; 3-4 strongly polluted ; 4-5 strongly to extremely polluted ; >5 extremely polluted.

ISSN No. 2321-2705 | DOI: 10.51244/IJRSI |Volume XIII Issue VI June 2026

Contamination Factor (CF)

CF quantifies contamination relative to background values (Hakanson, 1980) (equation 5) :

$$CF = {C_m}/{B_m} \quad (5)$$

Where C_m is the measured concentration ; B_m the background concentration. CF classes : <1 low ; 1-3 moderate ; 3-6 considerable ; >6 very high.

Single Pollution Index (PI)

PI uses tolerable guidelines (Kloke, 1979) (equation 6) :

$$PI = {C_n}/{GB} \quad (6)$$

Where C_n is the heavy metal content ; G_B the geochemical background values (Kloke, 1979). PI classes : <0.7 unpolluted ; 0.7-1.0 mildly polluted ; 1.0-2.0 moderately polluted ; 2.0-3.0 moderately to strongly polluted ; 3.0-5.0 strongly polluted ; >5.0 extremely polluted.

Pollution Load Index (PLI)

PLI provides a summative contamination assessment (Tomlinson et al., 1980) (equation 7) :

$$PLI = \sqrt[n]{PI_1 + PI_2 + \cdots PI_n} \quad (7)$$

Where PI are the values from equation 6, n the number of metals. PLI >1 indicates pollution.

Vector Modulus of Pollution Index (PIVector)

Introduced by Gong et al. (2008) (equation 8) :

$$PIVector = \sqrt{\frac{1}{n}\sum_{i-1}^{n} PI^2} \quad (8)$$

Multi-element Contamination (MEC)

MEC assesses anthropogenic impact (Adamu & Nganje, 2010) (equation 9) :

$$MEC = {(C_1/T_2 + C_2/T_2 + \cdots C_n/T_n)}/{n} \quad (9)$$

Where C_i is the metal concentration ; T_i the tolerable levels (Kloke, 1979) and n the number of metals. MEC >1 indicates anthropogenic impact.

Contamination Security Index (CSI)

CSI incorporates ERL and ERM values (Long et al., 1995 ; Pejman et al., 2015) (equation 10) :

$$CSI = \sum_{i-1}^{n} w\left(\left(\frac{C}{ERL}\right)^{1/2} + \left(\frac{C}{ERM}\right)^{2}\right) \quad (10)$$

Where w_i is the computed weight of each heavy metal (Pejman et al., 2015) ; C_i the metal concentration ; ERL thr effects range low and ERM the effects range median.

ISSN No. 2321-2705 | DOI: 10.51244/IJRSI |Volume XIII Issue VI June 2026

Degree of Contamination (Cdeg)

Summation of contamination factors (Hakanson, 1980) (equation 11) :

$$C_{deg} = \sum_{i-1}^{n} C_f \quad (11)$$

C_{deg} classes : <8 low ; 8-16 moderate ; 16-32 considerable; >32 very high.

Nemerow Pollution Index (IN)

Integrated assessment (Gong et al., 2008; Gao et al., 2016) (equation 12) :

$$IN = \sqrt{(P_{ia})^2 + (P_{im})^2}\Big/_2 \quad (12)$$

Where P_{ia} is the average single pollution index and P_{im} the maximum single pollution index. IN classes: <0.7 unpolluted; 0.7-1.0 slightly polluted; 1.0-2.0 moderately polluted; 2.0-3.0 heavily polluted; >3.0 extremely polluted.

Potential Ecological Risk Index (RI)

Hakanson's ecological risk (Hakanson, 1980) (equations 13-14) :

$$E_f^i = C_f^i \times T_f^i \quad (13)$$

$$RI = \sum_{i=1}^{n} E_f^i \quad (14)$$

Where T_f^i is the toxicity coefficient: Cu (5), Pb (5), Zn (1), Ni (5), Cr (2), As (10) (Zhao et al., 2005). RI classes: <40 low; 40-80 moderate; 80-160 considerable; 160-320 high; >320 very high.

Exposure Factor (ExF)

Assesses heavy metal load location (Babelewska, 2010) (equation 15) :

$$ExF = \sum_{i=1}^{n} C_n - C_{av}\Big/_{C_{av}} \quad (15)$$

Where C_n is the content at sampling point and C_{av} the average content of heavy metal.

Modified Degree of Contamination (mCd)

Integrated assessment (Abrahim & Parker, 2008) (equation 16) :

$$mCd = \sum_{i=1}^{n} C_n\Big/_n \quad (16)$$

mCd classes: <1.5 low; 1.5-2.0 moderate; 2.0-4.0 high; 4.0-8.0 very high; 8.0-16.0 extremely high; >16.0 ultra-high.

Human Health Risk Assessment

Quantitative human health risk assessment was conducted following USEPA standard frameworks (USEPA, 1989, 2001) to evaluate non-carcinogenic and carcinogenic risks from heavy metal exposure in soil.

Exposure Assessment

Three exposure pathways were considered: (1) direct soil ingestion; (2) dermal contact; (3) inhalation of soil

ISSN No. 2321-2705 | DOI: 10.51244/IJRSI |Volume XIII Issue VI June 2026

particles. Chronic Daily Intake (CDI, mg/kg-day) was calculated using equations 17-19 :

Ingestion:

$$CDI_{ing} = \frac{C \times IR \times EF \times ED}{BW \times AT} \times 10^{-6} \quad (17)$$

Dermal contact:

$$CDI_{dermal} = \frac{C \times SA \times AF \times ABS \times EF \times ED}{BW \times AT} \times 10^{-6} \quad (18)$$

Inhalation:

$$CDI_{dermal} = \frac{C \times IR_{air} \times EF \times ED}{BW \times AT \times PEF} \times 10^{-6} \quad (19)$$

Where: C is the metal concentration in soil (mg/kg); IR the ingestion rate (children 200 mg/day, adults 100 mg/day); EF the exposure frequency (365 days/year); ED the exposure duration (children 6 years, adults 30 years); BW the body weight (children 15 kg, adults 70 kg); AT the averaging time (ED × 365 days for non-carcinogens; 70 years × 365 days = 25,550 days for carcinogens); SA the skin surface area (children 1,600 cm^2, adults 5,800 cm^2); AF the adherence factor (children 0.2 mg/cm^2-day, adults 0.07 mg/cm^2-day); ABS the dermal absorption factor (0.001 for metals); IR_{air} the inhalation rate (children 5 m^3/day, adults 15 m^3/day) and PEF the particle emission factor (1.36 × 10^9 m^3/kg).

Non-Carcinogenic Risk

Hazard Quotient (HQ) for each metal and pathway was calculated (equation 20) :

$$HQ = \frac{CDI}{RfD} \quad (20)$$

Where RfD is the reference dose (mg/kg-day) (USEPA, 2023): As (0.0003 ingestion, 0.0003 dermal, 0.0003 inhalation); Pb (0.0035 ingestion, 0.0035 dermal, 0.0035 inhalation); Cu (0.04 ingestion, 0.04 dermal, 0.04 inhalation); Zn (0.3 ingestion, 0.06 dermal, 0.3 inhalation); Ni (0.02 ingestion, 0.02 dermal, 0.0006 inhalation); Cr (0.003 ingestion, 0.000075 dermal, 0.000005 inhalation); Fe (0.7 ingestion, 0.05 dermal, 0.7 inhalation).

Hazard Index (HI) was calculated as sum of HQs for all pathways (equation 21) :

$$HI = \sum HQ_{ing} + HQ_{dermal} + HQ_{inh} \quad (21)$$

HI >1 indicates potential non-carcinogenic health effects.

Carcinogenic Risk

Cancer risk (CR) was calculated for carcinogenic metals (As, Cr, Pb) (equation 22) :

$$CR = CDI_{ing} \times SF_{ing} + CDI_{dermal} \times SF_{dermal} + CDI_{inh} \times SF_{inh} \quad (22)$$

Where SF is the slope factor $(mg/kg\text{-}day)^{-1}$ (USEPA, 2023): As (1.5 ingestion, 3.66 dermal, 15.1 inhalation); Pb (0.0085 ingestion, 0.0085 dermal); Cr (0.5 ingestion, 0.5 dermal).

Statistical Analysis

Descriptive Statistics

Mean, median, standard deviation, minimum, and maximum values were calculated for all parameters using Microsoft Excel (2016).

Principal Component Analysis (PCA)

PCA was performed using Statistica 13 (TIBCO Software Inc.) to identify metal associations and potential contamination sources. Data were standardized (Z-scores) before analysis to eliminate scale effects. Eigenvalues >1 were retained (Kaiser criterion), and Varimax rotation was applied to simplify factor interpretation.

Correlation Analysis

Pearson correlation coefficients were calculated to assess relationships among metals and soil properties. Correlation significance was tested at $p < 0.05$ and $p < 0.01$ levels.

Cluster Analysis

Hierarchical agglomerative cluster analysis (Ward's method with squared Euclidean distance) was performed to group sampling locations by contamination profiles. The dendrogram was cut at 65% similarity to identify distinct contamination clusters.

Spatial Analysis

Kriging Interpolation : Spatial distribution maps were generated using Surfer 21 (Golden Software LLC) using ordinary kriging interpolation. Experimental variograms were fitted using weighted least squares regression. Variogram models were selected based on minimum residual sum of squares and cross-validation statistics (mean error and root mean squared standardized error). Spherical, exponential, and Gaussian models were tested for each metal, with the best-fit model selected for final interpolation.

Software

- **Microsoft Office 365 :** Data processing and calculations
- **ArcGIS Pro 3.0 (ESRI):** Map production (https://www.esri.com)
- **Google Earth Pro :** Location verification
- **Surfer 21 (Golden Software) :** Spatial interpolation and mapping
- **Statistica 13 (TIBCO) :** Statistical analysis (PCA, correlation, cluster analysis)

RESULTS

Descriptive Statistics of Heavy Metals

Heavy metal concentrations in the 30 soil samples are summarized in Table 2. The data show wide spatial variability, with coefficients of variation (CV) ranging from moderate (Cu: 36.3%, Fe: 70.2%) to very high (Pb: 156.2%, As: 200.0%, Cr: 102.3%).

Chromium (Cr) : Concentrations ranged from 0 to 457 mg/kg (mean 87 mg/kg). The highest concentration (457 mg/kg) was recorded at point E28 (Djengou washing station), exceeding WHO (100 mg/kg) and CSQG (87 mg/kg) limits. Zero values at locations E30 (abandoned mining site) and others were likely below detection limits (BDL <3 mg/kg) rather than true absence, as Cr is ubiquitous in crustal materials. The wide distribution suggests diffusible contamination spreading through industrial wastewater discharge. The presence of Cr may result from oxidation of ultramafic rocks or leaching of ultramafic soils, controlled by amorphous Fe-oxides (Garnier et al., 2009).

Copper (Cu) : Detected in all samples, concentrations ranged from 19 to 485 mg/kg (mean 272 mg/kg). All samples exceeded WHO (100 mg/kg), and 28 of 30 exceeded CSQG (63 mg/kg). High Cu retention is governed by ion exchange with kaolinite clays and complexation with humic/fulvic acids (Wu et al., 2002). The maximum

ISSN No. 2321-2705 | DOI: 10.51244/IJRSI |Volume XIII Issue VI June 2026

concentration (E18, Mboscoro) is attributed to Cu mobility in weathering environments and adsorption onto soil surfaces via ion exchange (Wuana et al., 2011). Similar findings were reported by Kabir et al. (2017) in Nigerian mine soils.

Lead (Pb) : Concentrations ranged from below detection (BDL <5 mg/kg) to 114 mg/kg (mean 16 mg/kg). Nine samples were BDL, likely true absence in undisturbed areas rather than analytical artifact. The maximum value (E8) exceeded WHO (85 mg/kg) and CSQG (70 mg/kg) limits. High Pb concentrations are attributable to mining activities, primarily from galena (PbS) weathering (Banunle et al., 2018). These values are significantly higher than those reported in South Africa (4.79 mg/kg; Caspah et al., 2016) and Ghana (19.96 mg/kg; Crentsil et al., 2016), but comparable to other Cameroonian gold mining areas (Dallou et al., 2018).

Zinc (Zn) : Concentrations ranged from BDL to 139 mg/kg (mean 23 mg/kg). While maximum values exceeded WHO (50 mg/kg), all were below CSQG (200 mg/kg). The highest value (E15) reflects inputs from both local and semi-mechanized mining activities. Zn concentrations were lower than those reported by Sijin et al. (2015) in China but higher than those from Sudan (Mushtaha et al., 2017).

Iron (Fe) : Extremely high concentrations compared to other metals, ranging from 8,550 to 121,611 mg/kg (mean 37,292 mg/kg). The mean was below WHO (50,000 mg/kg), but 9 of 30 samples exceeded this limit. High Fe concentrations reflect the ferralitic soil composition of the Kambele mining zone. The maximum value at E28 (121,611 mg/kg) is exceptionally high (≈2.4× WHO limit) and warrants verification due to potential measurement artifacts. Toxic effects related to Fe can appear at concentrations >50,000 ppm (WHO), affecting multiple organs, particularly in children (Baby et al., 2010 ; Chiroma et al., 2014).

Arsenic (As) : Concentrations ranged from BDL to 60 mg/kg (mean 7 mg/kg). Sixteen samples were BDL (<2 mg/kg). The maximum (E29) was three times the WHO limit (20 mg/kg). As presence is attributed to gold veins rich in arsenopyrite (FeAsS). These values exceed those reported by Dallou et al. (2018) for Batouri and Betare-Oya (4±2 mg/kg) but are comparable to Mominou et al. (2018).

Manganese (Mn) : Concentrations ranged from BDL to 885 mg/kg (mean 310 mg/kg). The mean exceeded Upper Continental Crust (UCC) values (600 mg/kg) and IASS limits (500 mg/kg). The maximum value (885 mg/kg) reflects natural enrichment from ferralitic soils. These results exceed those from Ghana (445.6 mg/kg ; Crentsil et al., 2016).

Nickel (Ni) : Concentrations ranged from 3.1 to 655.5 mg/kg (mean 162 mg/kg), with 26 of 30 samples exceeding WHO (50 mg/kg). The mean exceeds UCC (68 mg/kg). These values are higher than those from Batouri (Dallou et al., 2018) and China (Wang et al., 2019). The wide range indicates strong spatial heterogeneity and multiple contamination sources.

3.2 Physical-Chemical Properties

Table 4 summarizes physical parameters of soil samples.

pH: Ranged from 5.12 to 6.22 (mean 5.59), indicating acidic soils below WHO guidelines (6.5-8.5) but within IASS range (4-8.5). The acidic pH is explained by three mechanisms (equations 23-25) :

Oxidative decomposition of biotite minerals (Buss et al., 2008):

$$Na_{0.50}Ca_{0.48}K_{0.01}Al_{1.43}\,Si_{2.56}O_8 + 5.76\,H_2CO_3 + 2.24\,H_2O \rightarrow 0.50\,Na^+ + 0.48Ca^{2+} + 0.01K^+ + 1.43Al^{3+} + 2.56H_4SiO_4 + 5.76HCO_3^- \quad (23)$$

Non-oxidative mineral dissolution in acid medium (Crundwell, 2014):

$$\triangleright\, M_{lat} + wH_2O \rightleftharpoons M^{z+}_{(aq)} + \triangleright^{z-} \quad (24)$$

Sulfide oxidation producing sulfuric acid :

$$M_xS_y + 2yO_2 + yH_2O \longrightarrow M_xO_y + yH_2SO_4 \quad (25)$$

ISSN No. 2321-2705 | DOI: 10.51244/IJRSI |Volume XIII Issue VI June 2026

Acidic pH enhances metal mobility and bioavailability, promoting desorption of metal cations from tailings and waste materials. Conversely, under basic conditions, metal precipitation occurs:

$$M^{x+} + xHO^{-} \rightleftharpoons M(OH)_x \quad (26)$$

Electrical Conductivity (EC) : Ranged from 96 to 416 µS/cm (mean 213.3 µS/cm), indicating moderate salinity within tolerable limits (WHO 1000 µS/cm; IASS 40,000 µS/cm). Elevated EC suggests dissolution of mineral salts from mining operations.

Organic Matter (OM) : Ranged from 0.30 to 1.42% (mean 0.70%). Low OM values at E1, E8, E11, E17, and E22 reflect sandy soil textures. Higher OM at other locations enhances heavy metal retention through complexation (Gupta et al., 2007 ; Fijalkowski et al., 2012).

Moisture Content (MC) : Ranged from 1.30 to 18.81% (mean 9.49%), reflecting seasonal influences and hydrological conditions.

CONTAMINATION INTENSITY

Contamination Factor (CF)

CF values (Table 5) decreased in order : Cu (mean 6.1) > Ni (2.4) > Cr (1.0) > Pb (0.8) > As (0.5) > Zn (0.2). Soils showed significant enrichment in Cu and Ni (CF >3) and moderate enrichment in Cr (CF 1-3). High CF indicates external anthropogenic sources. These values exceed those reported by Dallou et al. (2018) in Batouri.

Enrichment Factor (EF)

EF values (Table 6) followed : Pb (mean 4.16) > Cu (4.71) > Ni (2.99) > Cr (1.75) > Zn (0.23) > As (0.08). Pb showed significant enrichment (EF 5-20), indicating strong anthropogenic influence. Cu and Ni showed moderate enrichment (EF 2-5), while Zn and As showed minimal enrichment. The mean EF <5 for all metals indicates moderate enrichment of the area, consistent with Dallou et al. (2018).

3.3.3 Pollution Indices (PI, PLI, IN, PIVector)

Table 7 presents pollution indices. PI values decreased : Cu (mean 6.1) > Ni (2.4) > Cr (1.0) > Pb (0.8) > As (0.5) > Zn (0.2), indicating mild to very high pollution for Cu and Ni. PLI ranged from 0.0-1.5, with three samples showing PLI >1, indicating local pollution. The mean PLI (0.2) suggests low overall pollution status (Mmolawa et al., 2011). IN values ranged from 2.3-8.1 (mean 4.7), indicating moderate to extreme contamination. Fourteen samples had IN >4, approaching extreme contamination ; 9 samples exceeded IN >5, indicating extreme contamination. These values exceed those from China (Wang et al., 2019), highlighting the severity of soil contamination.

Geo-accumulation Index (Igeo)

Igeo values (Table 8) decreased : Cu (mean 0.9) > Ni (0.3) > As (0.1) > Cr (0.0) > Zn (-0.4) > Pb (-0.1). Cu and Ni showed moderate contamination (Igeo 1-2), while others showed no or minimal contamination. These findings are consistent with Dallou et al. (2018) but lower than Obiora et al. (2016) in Nigeria.

Degree of Contamination (Cdeg and mCd)

C_{deg} (Table 9) ranged from 6.1 to 21.1 (mean 11.0), indicating moderate to considerable contamination. mCd ranged from 14.3 to 75.9 (mean 25.8), indicating very high to ultra-high contamination (Abrahim & Parker, 2008). The mCd values, which incorporate all metals simultaneously, highlight the cumulative impact of multiple contaminants.

Potential Ecological Risk (Ef and RI)

Table 10 presents ecological risk parameters. Ef values decreased : Cu (mean 30.3) > Ni (11.9) > As (5.5) > Pb (4.1) > Cr (1.9) > Zn (0.2). Cu showed moderate ecological risk (30-60), while others showed low risk. RI ranged from 26.7 to 127.5 (mean 53.8), with two samples showing RI >80 (considerable risk). These values are comparable to those reported by Jiang et al. (2014).

3.3.7 Contamination Security Index (CSI), MEC, and ExF

Table 11 presents CSI, MEC, and ExF values. CSI for Cu ranged from 2.94 to 979.58 (mean 351.67), indicating moderate to extreme contamination severity. Ni (mean 15.76) showed moderate severity, while Pb, Zn, Cr, and As showed low to moderate severity. MEC values (1.01-3.51, mean 1.83) >1 confirm anthropogenic contamination sources. ExF values (0.97-52.72, mean 10.71) identified E28 as the highest contamination hotspot.

STATISTICAL ANALYSIS

Correlation Analysis

Pearson correlation coefficients (Table S2) revealed significant positive correlations ($p < 0.05$) among : Cu-Cr (r=0.68), Cu-Pb (r=0.49), Cu-Ni (r=0.54), Cr-Ni (r=0.72), Cr-Pb (r=0.61), Fe-Mn (r=0.43), and As-Pb (r=0.38). These associations suggest common sources or similar geochemical behavior. Negative correlations were observed between Zn and Fe (r=-0.32) and Zn and Mn (r=-0.28), indicating different source contributions.

Principal Component Analysis (PCA)

PCA results (Figure 10) revealed three principal components explaining 72.83% of total variance :

PC1 (49.93%) : Positive loadings for Cu (0.82), Cr (0.79), Ni (0.74), Pb (0.68), and moderate positive for As (0.45). This component represents lithogenic sources influenced by natural pedogeochemical processes and mining-related inputs. The strong loadings of Cu-Cr-Ni-Pb suggest geogenic enrichment from weathering of ultramafic and granitic parent materials, enhanced by mining activities. Negative loadings for Zn (-0.52) and Fe (-0.41) indicate different source dynamics.

PC2 (22.90%) : Strong positive loadings for Fe (0.85) and Mn (0.79), with moderate negative loading for As (-0.38). This component represents ferralitic soil development and natural iron-manganese enrichment, typical of tropical weathering environments. The Fe-Mn association indicates sesquioxide accumulation under humid tropical conditions.

PC3 (12.07%) : Positive loadings for Zn (0.65) and Pb (0.44), representing localized anthropogenic inputs from specific mining activities (processing, transportation, waste disposal).

Cluster Analysis

Hierarchical cluster analysis (Ward's method) identified four contamination clusters (Figure S1) :

- **Cluster 1 (High contamination) :** E8, E18, E28 (Cu, Ni, Pb, As >90th percentile). These represent severe contamination hotspots requiring immediate remediation.
- **Cluster 2 (Moderate contamination) :** E1, E4, E6, E11, E15, E22, E24, E29 (moderate enrichment of multiple metals).
- **Cluster 3 (Low contamination) :** E9, E13, E16, E23, E30 (low metal concentrations, likely background sites).

ISSN No. 2321-2705 | DOI: 10.51244/IJRSI |Volume XIII Issue VI June 2026

- **Cluster 4 (Intermediate contamination) :** Remaining samples showing mixed profiles.

Spatial Analysis

Kriged interpolation maps (Figures 11-16) revealed heterogeneous contamination patterns across the Kambele mining area.

Arsenic (Figure 11) : Uneven distribution with high concentrations (>30 mg/kg) in the central-western portion near E29 (60 mg/kg) and E28 (50 mg/kg). These hotspots correspond to active processing areas, suggesting point-source contamination from arsenopyrite-rich ores.

Copper (Figure 12) : Wide distribution with very high concentrations (400-485 mg/kg) at E28 and E18. The contamination plume extends northward from processing areas, indicating lateral transport by surface runoff and potential groundwater mobilization.

Iron (Figure 13) : Exceptionally high concentrations at E28 (121,611 mg/kg) and E8 (89,000 mg/kg), coinciding with active mining zones. The elevated Fe reflects ferralitic soil composition and mobilization of Fe-oxides during mining operations.

Manganese (Figure 14) : Concentrations ranging from <100 to 885 mg/kg, with hotspots corresponding to Fe-rich areas, consistent with the Fe-Mn association observed in PCA.

Lead (Figure 15) : Patchy distribution with the highest concentration at E8 (114 mg/kg), isolated from other hotspots. This suggests a distinct Pb source, possibly related to historical galena-bearing materials or equipment contamination.

Zinc (Figure 16) : Highest concentrations (100-139 mg/kg) in the eastern sector (E15, E22, E24), potentially from agricultural inputs or specific mining activities.

Human Health Risk Assessment

Non-Carcinogenic Risk

Hazard Index (HI) values for children and adults are presented in Table 12. For children, HI >1 was observed at E8, E18, and E28 for As, Pb, and Cu exposure, indicating potential non-carcinogenic health risks. The highest HI for children was at E28 (HI = 3.42), primarily driven by As (HQ = 2.15) and Pb (HQ = 0.89). For adults, HI values were below 1 at all locations except E28 (HI = 1.12), reflecting lower exposure rates and higher body weight. Ingestion was the predominant exposure pathway (>85% of total HI), followed by dermal contact (10-12%) and inhalation (<3%).

Carcinogenic Risk

Cancer risk (CR) for As, Cr, and Pb exceeded the USEPA acceptable threshold (1×10^{-6}) at 12 sampling locations for children and 8 locations for adults. The highest CR was for As at E28 (CR = 3.6×10^{-5}), followed by Cr at E28 (CR = 1.8×10^{-5}). These elevated CR values indicate potentially unacceptable cancer risks, particularly for children, and warrant urgent intervention.

DISCUSSION

Contamination Sources and Mechanisms

The integration of PCA, correlation analysis, and spatial mapping provides robust source identification for heavy metal contamination in Kambele. Three primary sources were identified :

Source 1 (PC1, 49.93%) : Natural pedogeochemical background enhanced by mining. The Cu-Cr-Ni-Pb association reflects both lithogenic inheritance from granitic and ultramafic parent materials and mining-induced

mobilization. These metals are enriched in the Pan-African granitoids and schists characteristic of the Eastern Cameroon gold district (Tchouankam et al., 2020). Mining operations enhance their mobility through : (i) physical comminution increasing reactive surface areas ; (ii) acid generation from sulfide oxidation (equation 25) ; (iii) organic acid weathering from decomposing vegetation and mine wastes (Kong et al., 2014; Lazo et al., 2017).

Source 2 (PC2, 22.90%) : Ferralitic soil development. The Fe-Mn association represents natural geochemical processes characteristic of humid tropical environments. Ferrallitization involves intense weathering, desilication, and accumulation of Fe and Mn sesquioxides. These oxides act as effective scavengers for trace metals through adsorption and co-precipitation (Kabata-Pendias, 2011). The negative correlation of As with PC2 suggests that As is preferentially mobilized or not effectively retained by Fe-Mn oxides under acidic conditions.

Source 3 (PC3, 12.07%) : Localized anthropogenic inputs. Zn and moderate Pb enrichment at specific sites reflect contamination from : (i) Zn-containing fertilizers (guano application in agricultural areas); (ii) equipment and machinery wear (oil, grease, and metal parts); (iii) galvanized materials used in mining infrastructure; (iv) waste disposal practices.

Comparison with Regional and Global Mining Sites

Table 3 provides comparison of Kambele concentrations with other gold mining areas. The data demonstrate that Kambele contamination levels are generally intermediate to high but comparable to other artisanal gold mining sites.

Compared to Ghana (Crentsil et al., 2016) : Kambele has lower Fe (37,292 vs 531,500 mg/kg) and Mn (310 vs 445 mg/kg), but higher Cu (272 vs 16 mg/kg), Ni (162 vs 41.8 mg/kg), and Pb (16 vs 20 mg/kg). This reflects differences in geology (ferralitic soils vs Birimian formations) and mining intensity.

Compared to South Africa (Caspah et al., 2016) : Kambele shows higher Pb (16 vs 4.8 mg/kg) but lower Cr (87 vs 279 mg/kg) and Ni (162 vs 112 mg/kg). The Witwatersrand basin is characterized by quartz-pebble conglomerates with different metal associations.

Compared to Sudan (Mushtaha et al., 2017) : Kambele has higher Pb, Zn, Cu, Ni, and Fe, reflecting more intense mining activity and different geological context.

Compared to other Cameroon sites (Dallou et al., 2018 ; Mominou et al., 2018; Tehna et al., 2019; Mambou et al., 2020): Kambele shows higher Cu and Ni concentrations than most, comparable Pb levels, and lower Fe than some. The differences are attributable to local geology (Kambele's granitic-gneissic basement with sulfide-rich quartz veins), mining intensity (longer history and more extensive operations), and sample matrix (soil vs sediments).

Mechanisms of Metal Mobilization

Three reaction types explain elevated metal concentrations in Kambele soils :

Oxidative decomposition of minerals (Equation 23) : Biotite and other ferromagnesian minerals undergo oxidation in acid soils, releasing cations (Na^+, Ca^{2+}, Al^{3+}, K^+) and producing silicic acid. This process is enhanced by mining operations that expose fresh surfaces to oxidizing conditions.

Non-oxidative dissolution (Equation 24) : Mineral surfaces interact with water and organic acids, forming ionic species through bond-breaking. The Helmholtz double layer at mineral-water interfaces facilitates transfer of charged species, promoting metal release (Crundwell, 2014).

Organic acid weathering : Kandic minerals in ferralitic soils are weathered by organic acids (formic, oxalic, citric, tartaric acids) abundant in OM (1.42% max). These acids simultaneously promote acid attack and chelation of metal ions (Lazo et al., 2017), enhancing metal mobilization and availability. Seasonal variations

ISSN No. 2321-2705 | DOI: 10.51244/IJRSI |Volume XIII Issue VI June 2026

significantly affect these processes. During wet seasons (March-November), increased rainfall promotes acid generation, metal leaching, and transport ; during dry seasons (November-March),

Environmental and Health Implications

The acidic pH (5.12-6.22) enhances heavy metal bioavailability, posing direct risks to : (i) agricultural productivity and food safety ; (ii) groundwater quality; (iii) ecosystem health; (iv) human populations, particularly vulnerable groups (children, pregnant women, agricultural workers). Quantitative health risk assessment (Section 3.6) confirms potentially unacceptable non-carcinogenic and carcinogenic risks at multiple locations, particularly for children.

The presence of As, Pb, and Cr(VI) (toxic form) at concentrations exceeding WHO limits is of particular concern given their carcinogenic classification (Group 1 : As ; Group 2A : Pb; Group 3: Cr(VI)). The predicted cancer risks (3.6×10^{-5} for As at E28) exceed USEPA acceptable levels (1×10^{-6} to 1×10^{-4}), indicating a need for immediate intervention.

Climate change considerations : Projected increases in rainfall intensity (IPCC, 2022) could enhance metal leaching and transport, expanding contamination plumes and increasing risks to downstream water resources and agricultural areas. The Kambele region (humid tropical) is particularly vulnerable to such impacts.

STUDY LIMITATIONS

Several limitations should be acknowledged :

1. **Temporal scope :** Single-season sampling (June 2021) does not capture seasonal variability in metal mobility and concentration.

2. **Spatial coverage :** While 30 samples are appropriate for preliminary assessment, more detailed sampling (100+ points) would refine spatial patterns and statistical confidence.

3. **Analytical methodology :** XRF provides total concentrations but not speciation, limiting assessment of bioavailability. Future studies should include sequential extraction or DGT techniques.

4. **Backgrounds valus :** Using global averages (Taylor & McLennan, 1985) rather than local baseline values may overestimate contamination if natural concentrations exceed global averages. However, comparison with similar Cameroon sites (Table 3) supports our interpretations.

5. **Health risk assessment :** Conservative exposure parameters and deterministic approach may overestimate risks compared to probabilistic assessments. However, the identified risks remain significant.

Remediation Recommendations

Based on contamination types and magnitudes, site-specific remediation strategies are recommended :

For moderately contaminated areas (Cluster 3, Cluster 4) :

- **Phytoremediation :** Hyperaccumulators (e.g., Vetiveria zizanioides for Cu, Helianthus annuus for Pb, Pteris vittata for As) integrated with soil amendments. Estimated cost : $5,000-10,000/ha.

- **Soil amendments :** Lime application to raise pH (neutralizing acidity and reducing metal solubility); organic matter additions to complex metals; phosphate amendments to immobilize Pb and As.

For severely contaminated hotspots (Cluster 1 : E8, E18, E28) :

- **Excavation and off-site treatment :** Removal of highly contaminated soil (top 20-30 cm) for

ISSN No. 2321-2705 | DOI: 10.51244/IJRSI |Volume XIII Issue VI June 2026

treatment/disposal. Estimated cost : $50,000-100,000/ha.

- **In-situ immobilization :** Fe-Mn oxide amendments, biochar application, and pH adjustment to reduce bioavailability.

For all areas

- **Community health surveillance :** Regular monitoring of blood lead levels in children and pregnant women (recommended frequency : quarterly for high-risk zones).
- **Water quality monitoring :** Biweekly monitoring during wet season of surface and groundwater for As, Pb, Cu, Ni.
- **Agricultural guidance :** Restriction of crop cultivation in high-risk zones ; selection of low-accumulating crop varieties ; washing of vegetables before consumption.
- **Public awareness :** Education campaigns on safe practices (hand washing, avoiding soil ingestion, proper food preparation).

Policy Recommendations

1. **Regulatory interventions :** Enforce mining regulations (Cameroon Mining Code, 2016) requiring Environmental and Social Impact Assessments (ESIA) and implementation of Environmental Management Plans (EMP) for all mining operations, including artisanal activities.
2. **Monitoring programs :** Establish official monitoring network with monthly sampling of critical points (E8, E18, E28, E29, water intakes). Public reporting of results required.
3. **Community health surveillance :** Integrate with Ministry of Health to establish health screening programs in Batouri Health District. Focus on : (i) children <5 years : blood Pb, As ; (ii) pregnant women : blood Pb, As; (iii) miners: occupational exposure monitoring.
4. **Capacity building :** Train local health workers on heavy metal poisoning diagnosis and treatment ; provide chelation therapy supplies.
5. **Restoration fund :** Establish mine closure and site restoration fund financed by mining operators to cover long-term monitoring and remediation costs.

Decision Support Tools

To facilitate practical application, we propose :

1. **Contamination Severity Classification Map :** Combine multiple indices (IN, RI, mCd, CSI) to classify the study area into four risk zones (Table 13) :
   - Zone I (High risk, red) : >75th percentile of combined indices → immediate intervention required
   - Zone II (Medium-high risk, orange) : 50th-75th percentile → enhanced monitoring and targeted interventions
   - Zone III (Medium risk, yellow) : 25th-50th percentile → regular monitoring, precautionary measures
   - Zone IV (Low risk, green) : <25th percentile → baseline monitoring
2. **Decision Tree for Remediation Selection :** Based on (i) metal type and concentration ; (ii) land use ; (iii) accessibility ; (iv) cost constraints (Figure S2).

ISSN No. 2321-2705 | DOI: 10.51244/IJRSI |Volume XIII Issue VI June 2026

3. **Long-term Monitoring Plan :**

- **Frequency :** Quarterly (dry season : Jan, Feb ; wet season : Jun, Sep)
- **Parameters :** As, Pb, Cu, Ni, pH, EC, OM at all 30 points ; additional metals (Cd, Hg) annually
- **Locations :** Priority sites (E8, E18, E28, E29) monthly ; other sites quarterly
- **Responsibility :** Ministry of Environment, Nature Protection and Sustainable Development with independent third-party verification

CONCLUSION

This comprehensive assessment of soil quality in the Kambele gold mining area provides the first environmental baseline for this region, revealing significant heavy metal contamination with direct implications for human health and ecosystem integrity. Key findings include :

1. **Soil acidification :** Acidic pH (5.12-6.22) from sulfide oxidation and organic acid weathering enhances metal mobility and bioavailability, affecting agricultural suitability and contaminant transport.
2. **Severe contamination :** Multiple heavy metals (Pb, Cu, Ni, As, Fe, Zn) exceed WHO and CSQG guidelines, with Cu and Ni showing highest enrichment. The contamination is multi-elemental, reflecting both natural pedogeochemical enrichment and mining-related inputs.
3. **Three contamination sources :** PCA identified natural background (49.93%), ferralitic soil development (22.90%), and localized anthropogenic inputs (12.07%) as controlling metal distributions.
4. **Spatial heterogeneity :** Kriging maps revealed distinct hotspots (E28, E8, E18, E29) requiring priority remediation, and identified contamination plumes extending from processing areas.
5. **Health risks :** Quantitative health risk assessment indicates potential non-carcinogenic (HI >1) and carcinogenic (CR $>1\times10^{-6}$) risks at multiple locations, particularly for children, from As, Pb, and Cu exposure.
6. **Remediation needs :** Site-specific strategies are recommended, ranging from phytoremediation and soil amendments for moderate contamination to excavation and immobilization for severe hotspots, supported by community health surveillance and monitoring.

The findings underscore the urgent need for implementation of environmental management plans, stricter enforcement of mining regulations, and long-term monitoring programs to protect human health and environmental quality in the Kambele area. Future research should focus on : (i) seasonal variability in metal mobility ; (ii) metal speciation and bioavailability ; (iii) uptake into agricultural products ; (iv) effectiveness of remediation techniques under local conditions ; (v) health impact studies on exposed populations.

Conflict of Interest

The authors declare no conflicts of interest relevant to this study.

Acknowledgments

The authors thank the University of Ngaoundéré for logistical support and the local communities of Kambele for facilitating field access. No specific funding was received for this research.

Open Research

All data generated or analyzed during this study are included in this published article and its supplementary

information files. The software used are :

- Microsoft Office 365: Data processing and calculations
- ArcGIS Pro 3.0: Map production
- Google Earth Pro: Location verification
- Surfer 21 (Golden Software): Spatial interpolation and mapping
- Statistica 13 (TIBCO Software Inc.): Statistical analysis

REFERENCES

1. Abdullateef, J., Agbaji1, E.B., Ajibola1, V.O., Funtua, M.A., (2020). Application of Pollution Load Indices, Enrichment Factors,Contamination Factor and Health Risk Assessment of soils. Open J Anal Bioanal Chem. 4(1), 011-019.
2. Abhijit, M., Maiti, R., (2018). Geochemical contamination in the mine affected soil of Raniganj Coalfield–A river basin scale assessment. Geoscience Frontiers, 9(5), 1577-1590.
3. Abrahim, G.M.S., Parker, R. J., (2008). Assessment of heavy metal enrichment factors and the degree of contamination in marine sediments from Tamaki Estuary, Auckland, New Zealand. Environmental Monitoring and Assessment. 136, 227–238.
4. Adamu, C.I., Nganje, T.N., (2010). Heavy metal contamination of surface soil in relationship to land use patterns: A case study of Benue State, Nigeria. Materials Sciences and Applications. 1, 127–134.
5. Adenuga, A.A., Olufemi, D.A., Olajide, O.D., Eludoyin, A.O., Idowu, O.O., (2022). Environmental impact and health risk assessment of potentially toxic metals emanating from different anthropogenic activities related to E-wastes. Heliyon. 8(8), e10296.
6. Affum, A.O., Osae, S.D., Kwaansa-Ansah, E.E., Miyittah, M.K., (2020). Quality assessment and potential health risk of heavy metals in leafy and non-leafy vegetables irrigated with groundwater and municipal-waste-dominated stream in the Western Region, Ghana. Heliyon. Volume 6 (12), e05829.
7. Awasthi, G., Nagar, V., K.K., Rajput, V., Bauer, T., Srivastava, S., (2022). Sustainable Amelioration of Heavy Metals in Soil Ecosystem:Existing Developments to Emerging Trends. Minerals. 12, 85.
8. Axtmann, E.V., Luoma, S.N., (1991). Large-Scale Distribution of Metal Contamination in the Fine-Grained Sediments of the Clark Fork River, Montana, U.S.A. Applied Geochemistry . 6, 75-88.
9. Ayiwouo, M.N., Mambou, L.L.N., Takougang, S.K., Ngounouno, I., (2022). Spatio-temporal variation and assessment of trace metal contamination in sediments along the Lom River in the gold mining site of Gankombol (Adamawa Cameroon). Environmental Earth Sciences. 81(379), 1-20.
10. Babelewska, A., (2010). The impact of industrial emissions on heavy metal and sulphur contamination level within the area of the projected Jurassic National Park. Pra˛dnik Studies and Reports of the Prof Władysław Szafer Museum. 20, 135–145.
11. Baby, J., Raj, J.S., Biby, E.T., Sankarganesh, P., Jeevitha, M.V., Ajisha, S.U., Rajan, S.S., (2010). Toxic effect of heavy metals on aquatic environment. Int. J. Biol. Chem. Sci. 4, 939-952.
12. Bade, R., Oh, S., Shin, W., Hwang, I., (2013,). Human health risk assessment of soils contaminated with tal(loid)s by using DGT uptake: A case study of a former Korean metal refinery site. Hum.Ecol. Risk Assessment , 19, 767–777.
13. Baird, C., Michael, C., (2012). Environmental chemistry. Fifth Edition. Macmillan Higher Education.
14. Baker, D.E., Alloway, B.J., (2000). Analysis of heavy metals in soil. Int. J. Agric. Policy Res. 1(2), 151-196.
15. Bhargava, A., Carmona, F.F., Bhargava, M., Srivastava, S., (2012.). Approachesforenhanced phytoextractionofheavymetals. J.Environ.Manage. 105,103–120.
16. Banunle, A., Fei-Baffoe, B., Otchere, K.G., (2018). Determination of the Physico-Chemical Properties and Heavy Metal Status of the Tano River along the Catchment of the Ahafo Mine in the Brong-Ahafo Mine. Ghana. J Environ Anal Toxicol. 8(3), 2-11.
17. Brady D, Duncan J.R., (1994). Bioaccumulation of metal cations by Saccharomyces cerevisiae. Applied Microbiology and Biotechnology. 41, 149-154.

18. Buss, H.L., Sak, P.B., Webb, S.M., Brantley, S.L., (2008). Weathering of the Rio Blanco quartz diorite, Luquillo Mountains, Puerto Rico: Coupling oxidation, dissolution, and fracturing. Geochimica et Cosmochimica Acta 72, 4488-4507.
19. Caeiro, S., Costa, M.H., Ramos, T.B., Fernandes, F., Silveira, N., Coimbra, A., Painho, M., (2015). Assessing heavy metal contamination in Sado Estuary sediment: An index analysis approach. Ecol. Indicators. 5, 151-169.
20. Carter, M.R., Gregorich E.G., (2008). Soil Sampling and Methods of Analysis. Second Edition, CRC Press Taylor & Francis Group. 1-173.
21. Caspah, K.M., Manny, M., Morgan, M., (2016). Health risk assessment of heavy metals in soils from witwatersrand gold mining basin, South Africa. Int.J. Environ. Res. Public Health. 13, 663.
22. Castaing, C. Feybesse, J.L., Thiéblemont, D., Triboulet, C., Chèvremont, P., (1994). Palaeogeographical reconstructions of the Pan-African/Brasiliano orogen: closure of an oceanic domain or intracontinental convergence between major blocks. Precambrian Research. 69, 1-4.
23. Cazalet, M.L., (2012). Caractérisation physico-chimique d'un sédiment marin traité aux liants hydrauliques : Évaluation de la mobilité potentielle des polluants inorganiques. Thèse de Doctorat de l'Institut National des Sciences Appliquées de Lyon, 1-226.
24. Chiffoleau, J.F., Claisse, D., Cossa, D., Ficht, A., Gonzalez, J.L., Guyot, T., Michel, P., Miramand, P., Oger, C., Petit, F., (2001) La contamination métallique. Programme scientifique Seine-Aval, 8-La contamination métallique. ALT Brest, 1-39.
25. Chiroma, T.M., Ebewele, R.O., Hymore, F.K., (2014). Comparative assessement of heavy metal levels in soil, vegetables and urban grey waste water used for irrigation in Yola and Kano. Int.Ref. J. Eng. Sci. 3: 1-9.
26. Chukwu, A., Oji, K., (2018). Assessment of Pb, Zn, As, Ni, Cu, Cr and Cd in Agricultural Soils around Settlements of Abandoned Lead-Zinc Mine in Mkpuma Ekwoku, South-eastern, Nigeria. J. Appl. Sci. Environ. Manage. 22 (9) 1485 –1488.
27. Cossa, D., (1989). Cadmium in Mytilus Spp: Worldwide Survey and Relationship between seawater and Mussel Content. Marine environmental research. 26(4), 265-284.
28. Crentsil, B.K., EWUSI, A., (2016). Heavy metals contamination and human health risk assessment around Obuasi gold mine in Ghana. Environ. Monit. Assess. 188, 261-261.
29. Crundwell, F.K. (2014). The mechanism of dissolution of minerals in acidic and alkaline solutions: Part I - A new theory of non-oxidation dissolution. Hydrometallurgy 149, 252-264.
30. Csavina, J., Field, J., Taylor, M., Gao, S., Landázuri, A., Betterton, E., Sáez, A.E., (2012). A review on the importance of metals and metalloids in atmospheric dust and aerosol from mining operations. Sci. Total Environ. 433, 58–73.
31. Dallou, G.B., Louis, N., Abdourahimi, D. B., Saïdou, N.N.I., Boniface K., Godfroy K., (2018). Environmental Pollution by Heavy Metals in the Gold Mining. American Journal of Environmental Sciences. 14 (5), 212-225.
32. Dong, X., Li, C., Li, J., Wang, J., Liu, S., & Ye, B. (2010,). A novel approach for soil contamination assessment from heavy metal pollution: A linkage between discharge and adsorption. . J. Hazard. Mater. , 175, 1022–1030.
33. Emmanuel, A., Cobbina, S. J., Adomako, D., Duwiejuah, A. B., Asare, W., (2014). Assessment of heavy metals concentration in soils around oil filling and service stations in the Tamale Metropolis. Afri.J. Environ. Sci. Techn. 8, 256-266.
34. Ezeh H.N., Chukwu E., (2011). Small scale mining and heavy metals pollution of agricultural soil. Nig. J. Geol. Mining Res.3(4), 87-104.
35. Fijałkowski, K., Kacprzak, M., Grobelak, A., Placek, A., (2012). The Influence of Selected Soil Parameters on the Mobility of Heavy Metals in Soils. . Inzynieria i Ochrona Srodowiska. 5, 81-92.
36. Funoh, K. (2014). The impacts of artisanal gold mining on local livelihoods and the environ,ent in the forested areas of cameroun. Working paper 150. CIFOR. 25-26.
37. IARC Monographs on the Evaluation of Carcinogenic Risks to Humans (2012). Arsenic, Metals, Fibers and Dust. Vol. 100C. In: International Agency for Research on Cancer, Lyon, France, 46-53.
38. Gao, J., Du, F., Li, W., Han, J., Wang, X., Bao, J., Fan, A.P., (2016). Content and accumulation characteristics of heavy metals in dominant plants in Xiao Bai He Area of the Yellow River Wetland. . J Agro-Environ Sci. 35 (11), 2180–2186.

39. Garnier, J., Quantin, C., Echevarria, G., Becquer, T., (2009). Assessing chromate availability in tropical ultramafic soils using isotopic exchange kinetics. Journal of Soils and Sediments. 9(5), 468–475,.
40. Getaneh, W., Alemayehu, T., (2006). Metal contamination of the environment by placer and primary gold mining in the Adola region of southern Ethiopia. Environmental Geology, , 50(3), 339-352.
41. Gong, Q., Jun, D., Yunchuan, X., Qingfei, W., Liqiang, Y., (2008). Calculating pollution indices by heavy metals in ecological geochemistry assessment and a case study in parks of Beijing. Journal of China University of Geosciences. 19, 230–241.
42. Gupta, A.K., Sinha, S., (2007). Phytoextraction Capacity of the Plants Growing on Tannery Sludge Dumping Sites. Bioresource Technology. 98, 1788-1794.
43. Gyamfi, E., Appiah-Adjei, E.K., Adjei, K.A., (2019). potential heavy metal illution of soil and water resources from artisanal mining in Kokoteasua, Ghana. ground water for sustainable development, 8,450-456.
44. Hakanson, L., (1980). An Ecological Risk Index for Aquatic Pollution Control, a Sediment-Ecological Approach. Water. 14, 975-1001.
45. Jamilu, S.E., Ntale, M., Origa, H.O., (2014). Physico-Chemical Characteristics of Copper Tailings and Pyrite Soils in Western Uganda: Implication for Phytoremediation.. International Journal of Environmental Monitoring and Analysis. 2(4), 191-198.
46. Jiang, X., Lu, W.X., Zhao, H.Q., Yang, Q.C., Yang, Z.P., (2014). Potential ecological risk assessment and prediction of soil heavy-metal pollution around coal gangue dump. Nat. Hazards Earth Syst. Sci.14, 1599–1610.
47. Kabir S.A., Hassan, M.S., Abbas, M.A., Kura, A.M., (2017). Assessment of heavy metals contamination of soil and water around abandoned Pb-Zn mines in Yelu, Alkaleri Local Government Area of Bauchi State, Nigeria. Research Journal of Public and Environmental Health, 4(5), 72-77.
48. Khan, M. N., Wasim, A.A., Sarwar, A., Rasheed, M.F., (2011). Assessment of heavy metal toxicants in the roadside soil along the N-5, national highway, Pakistan. . Environ. Monit. Assess. 182, 587–595.
49. Kim, H., Cho, K., Purev, O., Choi, N., Lee, J., (2022). Remediation of Toxic Heavy Metal Contaminated Soil by Combining aWashing Ejector Based on Hydrodynamic Cavitation and Soil Washing Process. Int. J. Environ.Res. Public Health. 19, 786.
50. Kloke, A. (1979). Content of arsenic, cadmium, chromium,fluorine, lead, mercury, and nickel in plants grown on contaminated soils, United Nations-ECE symposium, Geneva. 51–53.
51. Kong, M., Huang, L., Li, L., Zhang, Z., Zheng, S., Wang, M. (2014). Effects of oxalic acid and citric acids on the tree clays mineral after incubation. Apply clay science. 99, 207-124.
52. Lazo, D.E., Dyer, L.G. , Alorro, R.D., (2017). Silicate, phosphate and carbonate mineral dissolution behaviour in the presence of organic acids: A review. Minerals Engineering. 100, 115-123.
53. Lee, P.K., Yu, S., Jeong, Y.-J., Seo, J., Choi, S., & Yoon, B.-Y. (2019). Source identification of arsenic contamination in agricultural soils surrounding a closed Cu smelter, South Korea. . Chemosphere. 217, 183–194.
54. Léopold, E. N., Sabine, D. D., Jung, M. C., (2016). Physical and Metals Impact of Traditional Gold Mining on Soils in Kombo-Laka Area (Meiganga, Cameroon). International Journal of Geosciences. 7, 1102-1121.
55. Li, W., Wang, F., Yang, W., Cui, Y., Fan, A., Miao, C., (2017). Pollution assessment and source apportionment of heavy metals in NanHai Wetland soil of Baotou City. Ecology Environ Sci. , 26(11),1977–1984.
56. Long, E.R., MacDonald, D.D., Smith, S.L., Calder, F.D. (1995). Incidence of adverse biological effects within ranges of chemical concentrations in marine and estuarine. Environmental Management. 19, 81–97.
57. Lorenzo, F., Alonso, A., Pellicer, M.J., Pérez-Arlucea, M., (2007). Historical Analysis of Heavy Metal Pollution in Three Estuaries on the North Coast of Galicia (NW Spain). Environmental Geology. 52, 789-802.
58. Luo, T., Ding, Y., Sun, J., Zou, W., Zhou, F., (2018). Pollution characteristics and assessment of heavy metals in wetlandsoil in the area of northern Jiangsu Province. . Environ Chem.., 37(5), 984–993.
59. Mambou, N.L.L., Mache, J.R., Ayiwouo, N.M., Takougang, K.S., Abende, S.R.Y., Roukaiyatou, S., (2020). Caracterization of Mining Waste from the Betare-Oya Gold Area (East Cameroon) and an Adsorption Test by Sabga Smectite (North-West Cameroon). Scientifica . 1-12.

60. Mandeng, E.P.B., Bondjè-Bidjeck, L.M., Ekoa-Bessa, A.Z., Ntomb, Y.D., Wassouo-Wadjou, J., Edjengte-Doumo, E.P. Bitom D.L., (2019). Contamination and risk assessment of heavy metals, and uranium of sediments in two watersheds in Abiete-Toko gold district, Southern Cameroon. Heliyon. 5, (10), e02591.
61. Marta, M., Mapani, B.S., Kamona, A.F., Ružičić, S., Mapaure, I., Chimwamurombe, P.M., (2014). Assessment of agricultural soil by potentially toxic metals dispersed from improperly disposed tailings, Kombat mine. Namibia Journal of geochemical exploration. 144, 409-420.
62. Matini, L., Ongoka, P.R., Tathy, J.P., (2011). Heavy metals in soil on spoil heap of an abandaoned lead ore treatment plant SE Congo Brzzaville. African journal of environmental science and technology. 5(2), 89-97.
63. Mmaduakor, E.C., Umeh, C.T., Morah, J.E., Omokpariola, D.O., Ekwuofu, A.A., Onwuegbuokwu, S.S., (2022). Pollution status, health risk assessment of potentially toxic elements in soil and their uptake by gongronema latifolium in peri-urban of Ora-Eri, south-eastern Nigeria. Heliyon. 8(8), e10362.
64. Mmolawa, K B., Likuku, A.S., Gaboutloeloe, G.K.., (2011). Assessment of heavy metal pollution in soils along major roadside areas in Botswana. . African J.Environ. Sci. Technol. 5, 186-196.
65. Mokam, S., Aurelle, B., Tsikam, M.C., (2013). Impact de l'exploitation artisanale de l'or sur les populations de Kambele, région de l'Est Cameroun. Journal du CIMEC, 1-30.
66. Mominou, N., Al Issah, Y., Sarki, B., Kah, E. (2018). Physicochemical Characterisation of Soils at the Gold Exploitation Sites of Bétaré-Oya District in Cameroon and Pollution Evaluation. Open Journal of Inorganic Chemi. 81-90.
67. Mushtaha, A.L.İ., Elhagwa, A., Elfaki, J., Sulieman, M., (2017). Influence of the artisanal gold mining on soil contamination with heavy metals: A case study from Dar-Mali locality, North of Atbara, River Nile State. Sudan. Eurasian J. Soil Sci. 6, 28-36.
68. Benson, N.U., Adedapo, A.E., Fred-Ahmadu, O.H., Williams, A.B., Udosen, E.D., Ayejuyo, O.O., Olajire, A.A., (2018). New ecological risk indices for evaluating heavy metalscontamination in aquatic sediment: A case study of the Gulf of Guinea. Regional Studies in Marine Science . 18, 44–56.
69. Nzenti, J.P., Barbey, P., Macaudiere, J., Soba, D., (1988). Origin and evolution of the late Precambrian high-grade Yaounde gneisses (Cameroon). . Precambrian research. 38(2), 91-109.
70. Obiora, S.C., Chukwu, A., Toteu, S.F., Davies, T.C., (2016). Assesment of heavy metal contamination in soils around Lead (Pb) - Zinc (Zn) mining areas in Enyigba. Southeastern Nigeria. J. Geol. Soc. India. 87, 453-462.
71. Oyourou, J.N., McCrindle, R., Combrinck, S., Fourie, C.J.S., (2019). investigation of of Zn and Pb contamination of soil at the abandoned Ededale mine, amelodi (Pretoria South Africa) using a field portable spectrometer. Journal of southen african institute of miningg and metallurgy. 119(1), 55-62.
72. Pawan, K. (2012). Heavy Metals in Environment. Saarbrucken, Germany. First Edition. Lambert Academic Publishing GmbH and Co.
73. PCD. (2019). Plan Communal de Développement de Batouri. Commune de BATOURI BP 42.6-407.
74. Pejman, A., Bidhendi, G.N., Ardestani, M., Saeedi, M., Baghvand, A., (2015). A new index for assessing heavy metals contamination in sediments: A case study. Ecological Indicators. 58, 365–373.
75. Penaye, J., Hell, J.V., (2013). Abandoned artisanal mining sites of Eastern Cameroon: environmental problems and Cameroon legislation:. Yaounde: institute for geological and mining research. Environmental problems and Cameroon regulation. In Conférence Johannesburg.
76. Poidevin, A., Ngako, V., Nnange, J. M., & Njanko, T. (2003). Pan-African tectonic evolution in central and southern Cameroon: transpression and transtension during sinistral shear movements. Journal of African Earth Sciences, 36(3), 207-214.
77. Ramahlo, M. N. (2013). Physico-chemical and biological characterization of soils from selected farmlands around three mining sites in Phalaborwa, Limpopo province (Doctoral dissertation, University of Limpopo (Turfloop Campus)).
78. Rohde, R. A., Muller, R. A., (2015). Air pollution in China: mapping of concentrations and sources. PloS one.10(8), e0135749.
79. Rossman, T. G., (2003). Mechanism of arsenic carcinogenesis: an integrated approach. Mutation Research/Fundamental and Molecular Mechanisms of Mutagenesis,.533(1-2), 37-65.
80. Salati, S., Moore, F.,(2010). Assessment of heavy metal concentration in the Khoshk River water and sediment, Shiraz. Southwest Iran. Environmental monitoring and assessment.164(1), 677-689.

81. Sawant, S.Y., Pawar, R.R., Lee S.M., Cho M.H., (2017). Binder-free production of 3D N-doped porous carbon cubes for efficient Pb^{2+} removal through batch and fixed bed adsorption. J. Clean. Prod. 168, 290-301.
82. Sijin L., Wang, Y., Teng, Y., Yu, X., (2015). Heavy metal pollution and ecological risk assessment of the paddy soils near a zinc-lead mining area in Hunan. Environmental monitoring and assessment. 187(10), 1-12.
83. Singh, A., Harrison, A., (1985). Standardized principal components. International journal of remote sensing, , 6(6), 883-896.
84. Syed, R.H., Khanam, D., Adyel, T.M., Islam, M.S., Ahsan, M.A., Akbor, M.A. (2012). Assessment of Heavy Metal Contamination of Agricultural Soil around Dhaka Export Processing Zone (DEPZ). Bangladesh. Appl. Sci. 2, 584-601.
85. Tariq, J., Ahmad, N., Mashiatullah, A., (2018). Heavy Metals Contamination and Ecological Risk Assessment in Surface Sediments of Namal Lake, Pakistan. Polish journal of environmental studies, 27(2).
86. Taylor, S.R., McLennan, S.M., (1985). The Continental Crust: Its Composition and Evolution. Oxford.: Blackwell Scientific Publication.
87. Tchouankam, J. K., Bertrand, M. M., Elie-Constant, B., Bernard, T., Gilbert, N., François, A. Y. R., Jacques, K.J.E., (2020). Economic Potential of Gold in Batouri (Eastern Cameroon). Earth Science Research. 21-27.
88. Tchounwou, P.B., Yedjou, C.G., Patlolla, A.K., Sutton, D. J., (2012). Heavy metal toxicity and the environment. Molecular, clinical and environmental toxicology.133-164.
89. Tehna, N., Daniel, N. F., Jacques, E., Marc, M. E. J., Sylvie, N. T., Cheo, S. E., Paul, B., (2015). Impending Pollution of Betare Oya Opencast Mining Environment (Eastern Cameroon). Journal of Environmental Science and Engineering , 4 37-46.
90. Teixeira, R.A., de Souza, E.S., Ferreira, J.R., Fernandes, A.R., (2018). Potentially toxic elements in soils and contamination indices at the Serra Pelada gold mine, Para, Brazil. Bioscience Journal. 34(6), 1477-1487.
91. Tirmizi, S.A., Wattoo, F.H., Wattoo, M.H.S., Khokhar, M.N., Iqbal, J., (2005). Analytical investigation of soil inorganic elements in cotton cultivated areas of Vehari-Pakistan. Journal of the Chemical Society of Pakistan. 27(6), 606-610.
92. Tokar E.J., Benbrahim-Tallaa L., Ward J.M., Lunn R., Sams R.L., Waalkes M.P. (2010). Cancer in experimental animals exposed to arsenic and arsenic compounds. Crit. Rev. Toxicol. 40 (10), 912-927.
93. Tomlinson, D.L., Wilson, J.G., Harris, C.R., Jeffrey, D.W., (1980). Problems in the assessment of heavy-metal levels in estuaries and the formation of a pollution index. Helgoländer meeresuntersuchungen. 33(1), 566-575.
94. Toteu, S.F., Penaye, J., Djomani, Y.P. (2004). Geodynamic evolution of the Pan-African belt in central Africa with special reference to Cameroon. Canadian Journal of Earth Sciences. 41(1), 73-85.
95. USEPA. (2013). Toxicity Relationship Analysis Program (TRAP) version 1.22 United States Environmental Protection Agency, . Washington D.C., USA.: Division. Mid-Continent Ecology.
96. Van-Schmus, W.R., Oliveira, E.P., Da-Silva-Filho, A.F., Toteu, S.F., Penaye, J., Guimarães, I.P. (2008). Proterozoic links between the Borborema province, NE Brazil, and the central African fold belt. Geological Society, London, Special Publication. 294(1), 69-99.
97. Varol, M. (2011). Assessment of heavy metal contamination in sediments of the Tigris River (Turkey) using pollution indices and multivariate statistical techniques. Journal of Hazardous Materials. 195, 355–364.
98. Wang, X., Sun, Y., Li, S., Wang, H., (2019). Spatial distribution and ecological risk assessment of heavy metals in soil from the Raoyanghe Wetland, China. PLoS ONE , 14(8), e0220409.
99. Weihua, G., Liu, X., Liu, Z., Li, G., (2010). Pollution and Potential Ecological Risk Evaluation of Heavy Metals in the Sediments around Dongjiang Harbor, Tianjin. Procedia Environmental Sciences. 2, 729–736.
100. WHO. (1996.). Trace Elements in Human Nutrition and Health. Geneva, Switzerland. ISBN-13: 9241561734, 361.
101. Wu, J., West, L. J., Stewart, D.I., (2002). Effect of humic substances on Cu (II) solubility in kaolin-sand soil. Journal of Hazardous Materials. 94(3), 223-238.

102. Guan, Y., Shao, C., Ju, M., (2014). Heavy metal contamination assessment and partition for industrial and mining gathering areas. International journal of environmental research and public health. 11(7), 7286-7303.
103. Yu, L., Cheng, J., Zhan, J., Jiang, A., (2016). Environmental quality and sources of heavy metals in the topsoil based on multivariate statistical analyses: a case study in Laiwu City, Shandong Province, China. Natural Hazards. 81(3), 1435-1445.
104. Zhang, X., Zhou, T.F., Yang, X.F., Yin, H.Q., Xiao, Z.H., (2005). Study on assessment methods of heavy metal pollution in river sediments. J. Hefei Univ. Technol. 28, 1419-1423.
105. Zhao, Q., Qi-xin, X. U., Kai, Y., (2005). Application of Potential Ecological Risk Index in Soil Pollution of Typical Polluting Industries. Journal of Eastchina Normal University (Natural Science). 1, 110-115.
106. Zhou, J., Dang, Z., Cai, M., Liu, C., (2007). Soil heavy metal pollution around the Dabaoshan mine,China. International Journal of Environmental Research and Public Health. 588–594.
107. Abdullateef, J., Agbaji1, E.B., Ajibola1, V.O., Funtua, M.A., (2020). Application of Pollution Load Indices, Enrichment Factors,Contamination Factor and Health Risk Assessment of soils. Open J Anal Bioanal Chem. 4(1), 011-019.
108. Abhijit, M., Maiti, R., (2018). Geochemical contamination in the mine affected soil of Raniganj Coalfield–A river basin scale assessment. Geoscience Frontiers, 9(5), 1577-1590.
109. Abrahim, G.M.S., Parker, R. J., (2008). Assessment of heavy metal enrichment factors and the degree of contamination in marine sediments from Tamaki Estuary, Auckland, New Zealand. Environmental Monitoring and Assessment. 136, 227–238.
110. Adamu, C.I., Nganje, T.N., (2010). Heavy metal contamination of surface soil in relationship to land use patterns: A case study of Benue State, Nigeria. Materials Sciences and Applications. 1, 127–134.
111. Adenuga, A.A., Olufemi, D.A., Olajide, O.D., Eludoyin, A.O., Idowu, O.O., (2022). Environmental impact and health risk assessment of potentially toxic metals emanating from different anthropogenic activities related to E-wastes. Heliyon. 8(8), e10296.
112. Affum, A.O., Osae, S.D., Kwaansa-Ansah, E.E., Miyittah, M.K., (2020). Quality assessment and potential health risk of heavy metals in leafy and non-leafy vegetables irrigated with groundwater and municipal-waste-dominated stream in the Western Region, Ghana. Heliyon. Volume 6 (12), e05829.
113. Awasthi, G., Nagar, V., K.K., Rajput, V., Bauer, T., Srivastava, S., (2022). Sustainable Amelioration of Heavy Metals in Soil Ecosystem:Existing Developments to Emerging Trends. Minerals. 12, 85.
114. Axtmann, E.V., Luoma, S.N., (1991). Large-Scale Distribution of Metal Contamination in the Fine-Grained Sediments of the Clark Fork River, Montana, U.S.A. Applied Geochemistry . 6, 75-88.
115. Ayiwouo, M.N., Mambou, L.L.N., Takougang, S.K., Ngounouno, I., (2022). Spatio-temporal variation and assessment of trace metal contamination in sediments along the Lom River in the gold mining site of Gankombol (Adamawa Cameroon). Environmental Earth Sciences. 81(379), 1-20.
116. Babelewska, A., (2010). The impact of industrial emissions on heavy metal and sulphur contamination level within the area of the projected Jurassic National Park. Pra˛dnik Studies and Reports of the Prof Władysław Szafer Museum. 20, 135–145.
117. Baby, J., Raj, J.S., Biby, E.T., Sankarganesh, P., Jeevitha, M.V., Ajisha, S.U., Rajan, S.S., (2010). Toxic effect of heavy metals on aquatic environment. Int. J. Biol. Chem. Sci. 4, 939-952.
118. Bade, R., Oh, S., Shin, W., Hwang, I., (2013,). Human health risk assessment of soils contaminated with tal(loid)s by using DGT uptake: A case study of a former Korean metal refinery site. Hum.Ecol. Risk Assessment , 19, 767–777.
119. Baird, C., Michael, C., (2012). Environmental chemistry. Fifth Edition. Macmillan Higher Education.
120. Baker, D.E., Alloway, B.J., (2000). Analysis of heavy metals in soil. Int. J. Agric. Policy Res. 1(2), 151-196.
121. Bhargava, A., Carmona, F.F., Bhargava, M., Srivastava, S., (2012.). Approachesforenhanced phytoextractionofheavymetals. J.Environ.Manage. 105,103–120.
122. Banunle, A., Fei-Baffoe, B., Otchere, K.G., (2018). Determination of the Physico-Chemical Properties and Heavy Metal Status of the Tano River along the Catchment of the Ahafo Mine in the Brong-Ahafo Mine. Ghana. J Environ Anal Toxicol. 8(3), 2-11.
123. Brady D, Duncan J.R., (1994). Bioaccumulation of metal cations by Saccharomyces cerevisiae. Applied Microbiology and Biotechnology. 41, 149-154.

124. Buss, H.L., Sak, P.B., Webb, S.M., Brantley, S.L., (2008). Weathering of the Rio Blanco quartz diorite, Luquillo Mountains, Puerto Rico: Coupling oxidation, dissolution, and fracturing. Geochimica et Cosmochimica Acta 72, 4488-4507.
125. Caeiro, S., Costa, M.H., Ramos, T.B., Fernandes, F., Silveira, N., Coimbra, A., Painho, M., (2015). Assessing heavy metal contamination in Sado Estuary sediment: An index analysis approach. Ecol. Indicators. 5, 151-169.
126. Carter, M.R., Gregorich E.G., (2008). Soil Sampling and Methods of Analysis. Second Edition, CRC Press Taylor & Francis Group. 1-173.
127. Caspah, K.M., Manny, M., Morgan, M., (2016). Health risk assessment of heavy metals in soils from witwatersrand gold mining basin, South Africa. Int.J. Environ. Res. Public Health. 13, 663.
128. Castaing, C. Feybesse, J.L., Thiéblemont, D., Triboulet, C., Chèvremont, P., (1994). Palaeogeographical reconstructions of the Pan-African/Brasiliano orogen: closure of an oceanic domain or intracontinental convergence between major blocks. Precambrian Research. 69, 1-4.
129. Cazalet, M.L., (2012). Caractérisation physico-chimique d'un sédiment marin traité aux liants hydrauliques : Évaluation de la mobilité potentielle des polluants inorganiques. Thèse de Doctorat de l'Institut National des Sciences Appliquées de Lyon, 1-226.
130. Chiffoleau, J.F., Claisse, D., Cossa, D., Ficht, A., Gonzalez, J.L., Guyot, T., Michel, P., Miramand, P., Oger, C., Petit, F., (2001) La contamination métallique. Programme scientifique Seine-Aval, 8-La contamination métallique. ALT Brest, 1-39.
131. Chiroma, T.M., Ebewele, R.O., Hymore, F.K., (2014). Comparative assessement of heavy metal levels in soil, vegetables and urban grey waste water used for irrigation in Yola and Kano. Int.Ref. J. Eng. Sci. 3: 1-9.
132. Chukwu, A., Oji, K., (2018). Assessment of Pb, Zn, As, Ni, Cu, Cr and Cd in Agricultural Soils around Settlements of Abandoned Lead-Zinc Mine in Mkpuma Ekwoku, South-eastern, Nigeria. J. Appl. Sci. Environ. Manage. 22 (9) 1485 –1488.
133. Cossa, D., (1989). Cadmium in Mytilus Spp: Worldwide Survey and Relationship between seawater and Mussel Content. Marine environmental research. 26(4), 265-284.
134. Crentsil, B.K., EWUSI, A., (2016). Heavy metals contamination and human health risk assessment around Obuasi gold mine in Ghana. Environ. Monit. Assess. 188, 261-261.
135. Crundwell, F.K. (2014). The mechanism of dissolution of minerals in acidic and alkaline solutions: Part I - A new theory of non-oxidation dissolution. Hydrometallurgy 149, 252-264.
136. Csavina, J., Field, J., Taylor, M., Gao, S., Landázuri, A., Betterton, E., Sáez, A.E., (2012). A review on the importance of metals and metalloids in atmospheric dust and aerosol from mining operations. Sci. Total Environ. 433, 58–73.
137. Dallou, G.B., Louis, N., Abdourahimi, D. B., Saïdou, N.N.I., Boniface K., Godfroy K., (2018). Environmental Pollution by Heavy Metals in the Gold Mining. American Journal of Environmental Sciences. 14 (5), 212-225.
138. Dong, X., Li, C., Li, J., Wang, J., Liu, S., & Ye, B. (2010,). A novel approach for soil contamination assessment from heavy metal pollution: A linkage between discharge and adsorption. . J. Hazard. Mater. , 175, 1022–1030.
139. Emmanuel, A., Cobbina, S. J., Adomako, D., Duwiejuah, A. B., Asare, W., (2014). Assessment of heavy metals concentration in soils around oil filling and service stations in the Tamale Metropolis. Afri.J. Environ. Sci. Techn. 8, 256-266.
140. Ezeh H.N., Chukwu E., (2011). Small scale mining and heavy metals pollution of agricultural soil. Nig. J. Geol. Mining Res.3(4), 87-104.
141. Fijałkowski, K., Kacprzak, M., Grobelak, A., Placek, A., (2012). The Influence of Selected Soil Parameters on the Mobility of Heavy Metals in Soils. . Inzynieria i Ochrona Srodowiska. 5, 81-92.
142. Funoh, K. (2014). The impacts of artisanal gold mining on local livelihoods and the environ,ent in the forested areas of cameroun. Working paper 150. CIFOR. 25-26.
143. IARC Monographs on the Evaluation of Carcinogenic Risks to Humans (2012). Arsenic, Metals, Fibers and Dust. Vol. 100C. In: International Agency for Research on Cancer, Lyon, France, 46-53.
144. Gao, J., Du, F., Li, W., Han, J., Wang, X., Bao, J., Fan, A.P., (2016). Content and accumulation characteristics of heavy metals in dominant plants in Xiao Bai He Area of the Yellow River Wetland. . J Agro-Environ Sci. 35 (11), 2180–2186.

145. Garnier, J., Quantin, C., Echevarria, G., Becquer, T., (2009). Assessing chromate availability in tropical ultramafic soils using isotopic exchange kinetics. Journal of Soils and Sediments. 9(5), 468–475,.
146. Getaneh, W., Alemayehu, T., (2006). Metal contamination of the environment by placer and primary gold mining in the Adola region of southern Ethiopia. Environmental Geology, , 50(3), 339-352.
147. Gong, Q., Jun, D., Yunchuan, X., Qingfei, W., Liqiang, Y., (2008). Calculating pollution indices by heavy metals in ecological geochemistry assessment and a case study in parks of Beijing. Journal of China University of Geosciences. 19, 230–241.
148. Gupta, A.K., Sinha, S., (2007). Phytoextraction Capacity of the Plants Growing on Tannery Sludge Dumping Sites. Bioresource Technology. 98, 1788-1794.
149. Gyamfi, E., Appiah-Adjei, E.K., Adjei, K.A., (2019). potential heavy metal illution of soil and water resources from artisanal mining in Kokoteasua, Ghana. ground water for sustainable development, 8,450-456.
150. Hakanson, L., (1980). An Ecological Risk Index for Aquatic Pollution Control, a Sediment-Ecological Approach. Water. 14, 975-1001.
151. Jamilu, S.E., Ntale, M., Origa, H.O., (2014). Physico-Chemical Characteristics of Copper Tailings and Pyrite Soils in Western Uganda: Implication for Phytoremediation.. International Journal of Environmental Monitoring and Analysis. 2(4), 191-198.
152. Jiang, X., Lu, W.X., Zhao, H.Q., Yang, Q.C., Yang, Z.P., (2014). Potential ecological risk assessment and prediction of soil heavy-metal pollution around coal gangue dump. Nat. Hazards Earth Syst. Sci.14, 1599–1610.
153. Kabir S.A., Hassan, M.S., Abbas, M.A., Kura, A.M., (2017). Assessment of heavy metals contamination of soil and water around abandoned Pb-Zn mines in Yelu, Alkaleri Local Government Area of Bauchi State, Nigeria. Research Journal of Public and Environmental Health, 4(5), 72-77.
154. Khan, M. N., Wasim, A.A., Sarwar, A., Rasheed, M.F., (2011). Assessment of heavy metal toxicants in the roadside soil along the N-5, national highway, Pakistan. . Environ. Monit. Assess. 182, 587–595.
155. Kim, H., Cho, K., Purev, O., Choi, N., Lee, J., (2022). Remediation of Toxic Heavy Metal Contaminated Soil by Combining aWashing Ejector Based on Hydrodynamic Cavitation and Soil Washing Process. Int. J. Environ.Res. Public Health. 19, 786.
156. Kloke, A. (1979). Content of arsenic, cadmium, chromium,fluorine, lead, mercury, and nickel in plants grown on contaminated soils, United Nations-ECE symposium, Geneva. 51–53.
157. Kong, M., Huang, L., Li, L., Zhang, Z., Zheng, S., Wang, M. (2014). Effects of oxalic acid and citric acids on the tree clays mineral after incubation. Apply clay science. 99, 207-124.
158. Lazo, D.E., Dyer, L.G. , Alorro, R.D., (2017). Silicate, phosphate and carbonate mineral dissolution behaviour in the presence of organic acids: A review. Minerals Engineering. 100, 115-123.
159. Lee, P.K., Yu, S., Jeong, Y.-J., Seo, J., Choi, S., & Yoon, B.-Y. (2019). Source identification of arsenic contamination in agricultural soils surrounding a closed Cu smelter, South Korea. . Chemosphere. 217, 183–194.
160. Léopold, E. N., Sabine, D. D., Jung, M. C., (2016). Physical and Metals Impact of Traditional Gold Mining on Soils in Kombo-Laka Area (Meiganga, Cameroon). International Journal of Geosciences. 7, 1102-1121.
161. Li, W., Wang, F., Yang, W., Cui, Y., Fan, A., Miao, C., (2017). Pollution assessment and source apportionment of heavy metals in NanHai Wetland soil of Baotou City. Ecology Environ Sci. , 26(11),1977–1984.
162. Long, E.R., MacDonald, D.D., Smith, S.L., Calder, F.D. (1995). Incidence of adverse biological effects within ranges of chemical concentrations in marine and estuarine. Environmental Management. 19, 81–97.
163. Lorenzo, F., Alonso, A., Pellicer, M.J., Pérez-Arlucea, M., (2007). Historical Analysis of Heavy Metal Pollution in Three Estuaries on the North Coast of Galicia (NW Spain). Environmental Geology. 52, 789-802.
164. Luo, T., Ding, Y., Sun, J., Zou, W., Zhou, F., (2018). Pollution characteristics and assessment of heavy metals in wetlandsoil in the area of northern Jiangsu Province. . Environ Chem.., 37(5), 984–993.
165. Mambou, N.L.L., Mache, J.R., Ayiwouo, N.M., Takougang, K.S., Abende, S.R.Y., Roukaiyatou, S., (2020). Caracterization of Mining Waste from the Betare-Oya Gold Area (East Cameroon) and an Adsorption Test by Sabga Smectite (North-West Cameroon). Scientifica . 1-12.

166. Mandeng, E.P.B., Bondjè-Bidjeck, L.M., Ekoa-Bessa, A.Z., Ntomb, Y.D., Wassouo-Wadjou, J., Edjengte-Doumo, E.P. Bitom D.L., (2019). Contamination and risk assessment of heavy metals, and uranium of sediments in two watersheds in Abiete-Toko gold district, Southern Cameroon. Heliyon. 5, (10), e02591.
167. Marta, M., Mapani, B.S., Kamona, A.F., Ružičić, S., Mapaure, I., Chimwamurombe, P.M., (2014). Assessment of agricultural soil by potentially toxic metals dispersed from improperly disposed tailings, Kombat mine. Namibia Journal of geochemical exploration. 144, 409-420.
168. Matini, L., Ongoka, P.R., Tathy, J.P., (2011). Heavy metals in soil on spoil heap of an abandaoned lead ore treatment plant SE Congo Brzzaville. African journal of environmental science and technology. 5(2), 89-97.
169. Mmaduakor, E.C., Umeh, C.T., Morah, J.E., Omokpariola, D.O., Ekwuofu, A.A., Onwuegbuokwu, S.S., (2022). Pollution status, health risk assessment of potentially toxic elements in soil and their uptake by gongronema latifolium in peri-urban of Ora-Eri, south-eastern Nigeria. Heliyon. 8(8), e10362.
170. Mmolawa, K B., Likuku, A.S., Gaboutloeloe, G.K.., (2011). Assessment of heavy metal pollution in soils along major roadside areas in Botswana. . African J.Environ. Sci. Technol. 5, 186-196.
171. Mokam, S., Aurelle, B., Tsikam, M.C., (2013). Impact de l'exploitation artisanale de l'or sur les populations de Kambele, région de l'Est Cameroun. Journal du CIMEC, 1-30.
172. Mominou, N., Al Issah, Y., Sarki, B., Kah, E. (2018). Physicochemical Characterisation of Soils at the Gold Exploitation Sites of Bétaré-Oya District in Cameroon and Pollution Evaluation. Open Journal of Inorganic Chemi. 81-90.
173. Mushtaha, A.L.İ., Elhagwa, A., Elfaki, J., Sulieman, M., (2017). Influence of the artisanal gold mining on soil contamination with heavy metals: A case study from Dar-Mali locality, North of Atbara, River Nile State. Sudan. Eurasian J. Soil Sci. 6, 28-36.
174. Benson, N.U., Adedapo, A.E., Fred-Ahmadu, O.H., Williams, A.B., Udosen, E.D., Ayejuyo, O.O., Olajire, A.A., (2018). New ecological risk indices for evaluating heavy metalscontamination in aquatic sediment: A case study of the Gulf of Guinea. Regional Studies in Marine Science . 18, 44–56.
175. Nzenti, J.P., Barbey, P., Macaudiere, J., Soba, D., (1988). Origin and evolution of the late Precambrian high-grade Yaounde gneisses (Cameroon). . Precambrian research. 38(2), 91-109.
176. Obiora, S.C., Chukwu, A., Toteu, S.F., Davies, T.C., (2016). Assesment of heavy metal contamination in soils around Lead (Pb) - Zinc (Zn) mining areas in Enyigba. Southeastern Nigeria. J. Geol. Soc. India. 87, 453-462.
177. Oyourou, J.N., McCrindle, R., Combrinck, S., Fourie, C.J.S., (2019). investigation of of Zn and Pb contamination of soil at the abandoned Ededale mine, amelodi (Pretoria South Africa) using a field portable spectrometer. Journal of southen african institute of miningg and metallurgy. 119(1), 55-62.
178. Pawan, K. (2012). Heavy Metals in Environment. Saarbrucken, Germany. First Edition. Lambert Academic Publishing GmbH and Co.
179. PCD. (2019). Plan Communal de Développement de Batouri. Commune de BATOURI BP 42.6-407.
180. Pejman, A., Bidhendi, G.N., Ardestani, M., Saeedi, M., Baghvand, A., (2015). A new index for assessing heavy metals contamination in sediments: A case study. Ecological Indicators. 58, 365–373.
181. Penaye, J., Hell, J.V., (2013). Abandoned artisanal mining sites of Eastern Cameroon: environmental problems and Cameroon legislation:. Yaounde: institute for geological and mining research. Environmental problems and Cameroon regulation. In Conférence Johannesburg.
182. Poidevin, A., Ngako, V., Nnange, J. M., & Njanko, T. (2003). Pan-African tectonic evolution in central and southern Cameroon: transpression and transtension during sinistral shear movements. Journal of African Earth Sciences, 36(3), 207-214.
183. Ramahlo, M. N. (2013). Physico-chemical and biological characterization of soils from selected farmlands around three mining sites in Phalaborwa, Limpopo province (Doctoral dissertation, University of Limpopo (Turfloop Campus)).
184. Rohde, R. A., Muller, R. A., (2015). Air pollution in China: mapping of concentrations and sources. PloS one.10(8), e0135749.
185. Rossman, T. G., (2003). Mechanism of arsenic carcinogenesis: an integrated approach. Mutation Research/Fundamental and Molecular Mechanisms of Mutagenesis,.533(1-2), 37-65.
186. Salati, S., Moore, F.,(2010). Assessment of heavy metal concentration in the Khoshk River water and sediment, Shiraz. Southwest Iran. Environmental monitoring and assessment.164(1), 677-689.

187. Sawant, S.Y., Pawar, R.R., Lee S.M., Cho M.H., (2017). Binder-free production of 3D N-doped porous carbon cubes for efficient Pb^{2+} removal through batch and fixed bed adsorption. J. Clean. Prod. 168, 290-301.
188. Sijin L., Wang, Y., Teng, Y., Yu, X., (2015). Heavy metal pollution and ecological risk assessment of the paddy soils near a zinc-lead mining area in Hunan. Environmental monitoring and assessment. 187(10), 1-12.
189. Singh, A., Harrison, A., (1985). Standardized principal components. International journal of remote sensing, , 6(6), 883-896.
190. Syed, R.H., Khanam, D., Adyel, T.M., Islam, M.S., Ahsan, M.A., Akbor, M.A. (2012). Assessment of Heavy Metal Contamination of Agricultural Soil around Dhaka Export Processing Zone (DEPZ). Bangladesh. Appl. Sci. 2, 584-601.
191. Tariq, J., Ahmad, N., Mashiatullah, A., (2018). Heavy Metals Contamination and Ecological Risk Assessment in Surface Sediments of Namal Lake, Pakistan. Polish journal of environmental studies, 27(2).
192. Taylor, S.R., McLennan, S.M., (1985). The Continental Crust: Its Composition and Evolution. Oxford.: Blackwell Scientific Publication.
193. Tchouankam, J. K., Bertrand, M. M., Elie-Constant, B., Bernard, T., Gilbert, N., François, A. Y. R., Jacques, K.J.E., (2020). Economic Potential of Gold in Batouri (Eastern Cameroon). Earth Science Research. 21-27.
194. Tchounwou, P.B., Yedjou, C.G., Patlolla, A.K., Sutton, D. J., (2012). Heavy metal toxicity and the environment. Molecular, clinical and environmental toxicology.133-164.
195. Tehna, N., Daniel, N. F., Jacques, E., Marc, M. E. J., Sylvie, N. T., Cheo, S. E., Paul, B., (2015). Impending Pollution of Betare Oya Opencast Mining Environment (Eastern Cameroon). Journal of Environmental Science and Engineering , 4 37-46.
196. Teixeira, R.A., de Souza, E.S., Ferreira, J.R., Fernandes, A.R., (2018). Potentially toxic elements in soils and contamination indices at the Serra Pelada gold mine, Para, Brazil. Bioscience Journal. 34(6), 1477-1487.
197. Tirmizi, S.A., Wattoo, F.H., Wattoo, M.H.S., Khokhar, M.N., Iqbal, J., (2005). Analytical investigation of soil inorganic elements in cotton cultivated areas of Vehari-Pakistan. Journal of the Chemical Society of Pakistan. 27(6), 606-610.
198. Tokar E.J., Benbrahim-Tallaa L., Ward J.M., Lunn R., Sams R.L., Waalkes M.P. (2010). Cancer in experimental animals exposed to arsenic and arsenic compounds. Crit. Rev. Toxicol. 40 (10), 912-927.
199. Tomlinson, D.L., Wilson, J.G., Harris, C.R., Jeffrey, D.W., (1980). Problems in the assessment of heavy-metal levels in estuaries and the formation of a pollution index. Helgoländer meeresuntersuchungen. 33(1), 566-575.
200. Toteu, S.F., Penaye, J., Djomani, Y.P. (2004). Geodynamic evolution of the Pan-African belt in central Africa with special reference to Cameroon. Canadian Journal of Earth Sciences. 41(1), 73-85.
201. USEPA. (2013). Toxicity Relationship Analysis Program (TRAP) version 1.22 United States Environmental Protection Agency, . Washington D.C., USA.: Division. Mid-Continent Ecology.
202. Van-Schmus, W.R., Oliveira, E.P., Da-Silva-Filho, A.F., Toteu, S.F., Penaye, J., Guimarães, I.P. (2008). Proterozoic links between the Borborema province, NE Brazil, and the central African fold belt. Geological Society, London, Special Publication. 294(1), 69-99.
203. Varol, M. (2011). Assessment of heavy metal contamination in sediments of the Tigris River (Turkey) using pollution indices and multivariate statistical techniques. Journal of Hazardous Materials. 195, 355–364.
204. Wang, X., Sun, Y., Li, S., Wang, H., (2019). Spatial distribution and ecological risk assessment of heavy metals in soil from the Raoyanghe Wetland, China. PLoS ONE , 14(8), e0220409.
205. Weihua, G., Liu, X., Liu, Z., Li, G., (2010). Pollution and Potential Ecological Risk Evaluation of Heavy Metals in the Sediments around Dongjiang Harbor, Tianjin. Procedia Environmental Sciences. 2, 729–736.
206. WHO. (1996.). Trace Elements in Human Nutrition and Health. Geneva, Switzerland. ISBN-13: 9241561734, 361.
207. Wu, J., West, L. J., Stewart, D.I., (2002). Effect of humic substances on Cu (II) solubility in kaolin-sand soil. Journal of Hazardous Materials. 94(3), 223-238.

208. Guan, Y., Shao, C., Ju, M., (2014). Heavy metal contamination assessment and partition for industrial and mining gathering areas. International journal of environmental research and public health. 11(7), 7286-7303.
209. Yu, L., Cheng, J., Zhan, J., Jiang, A., (2016). Environmental quality and sources of heavy metals in the topsoil based on multivariate statistical analyses: a case study in Laiwu City, Shandong Province, China. Natural Hazards. 81(3), 1435-1445.
210. Zhang, X., Zhou, T.F., Yang, X.F., Yin, H.Q., Xiao, Z.H., (2005). Study on assessment methods of heavy metal pollution in river sediments. J. Hefei Univ. Technol. 28, 1419-1423.
211. Zhao, Q., Qi-xin, X. U., Kai, Y., (2005). Application of Potential Ecological Risk Index in Soil Pollution of Typical Polluting Industries. Journal of Eastchina Normal University (Natural Science). 1, 110-115.
212. Zhou, J., Dang, Z., Cai, M., Liu, C., (2007). Soil heavy metal pollution around the Dabaoshan mine,China. International Journal of Environmental Research and Public Health. 588–594.

ISSN No. 2321-2705 | DOI: 10.51244/IJRSI |Volume XIII Issue VI June 2026

FIGURE LIST

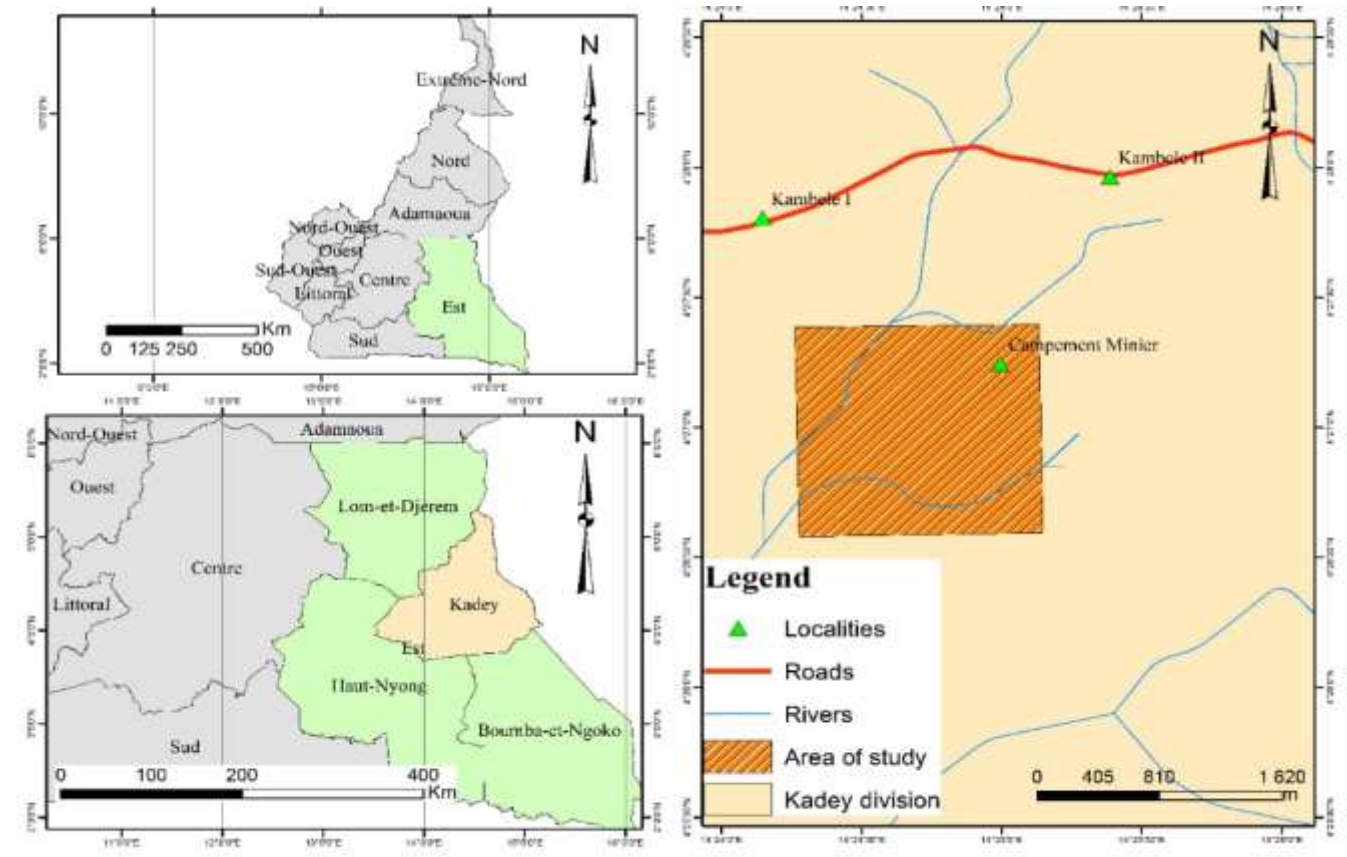

Figure 1: Location of Kambele Mining site.

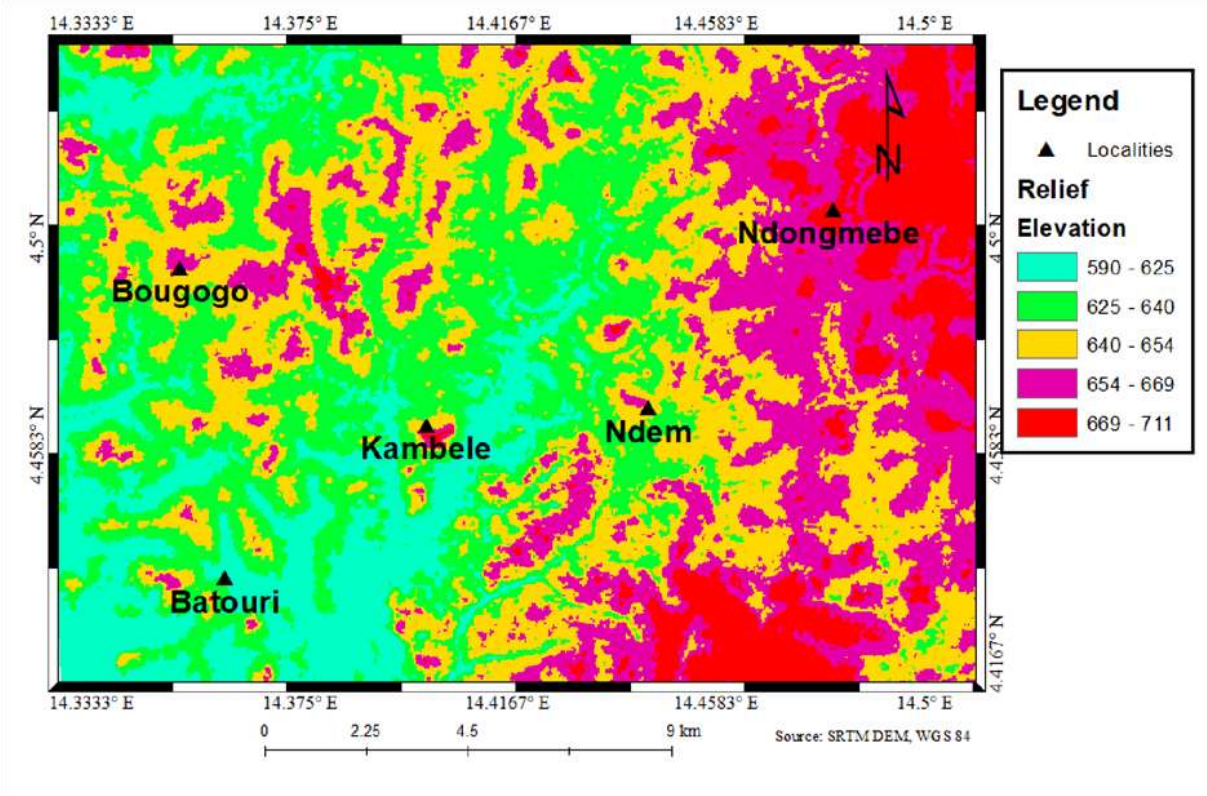

Figure 2: Topographic map of the Kambele Mining Zone.

ISSN No. 2321-2705 | DOI: 10.51244/IJRSI |Volume XIII Issue VI June 2026

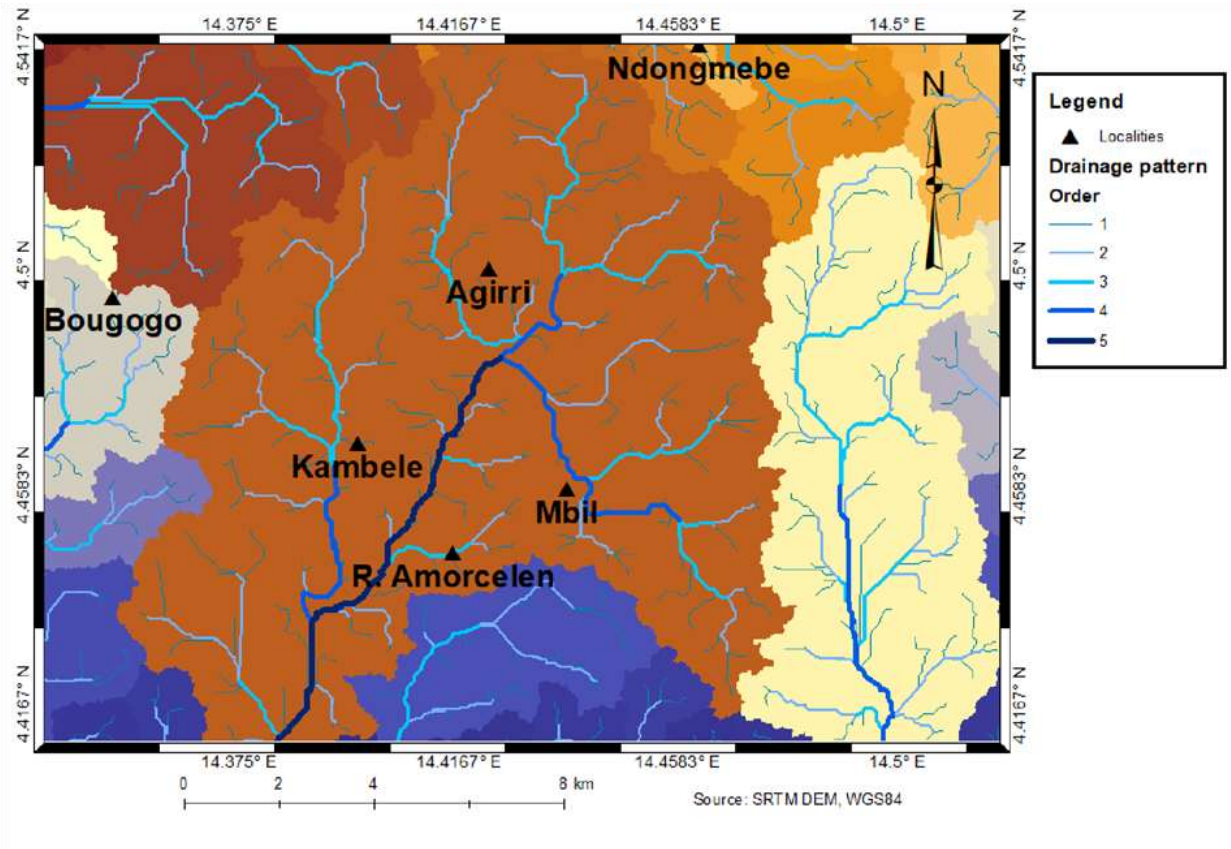

Figure 3: Hydrography of Kambele.

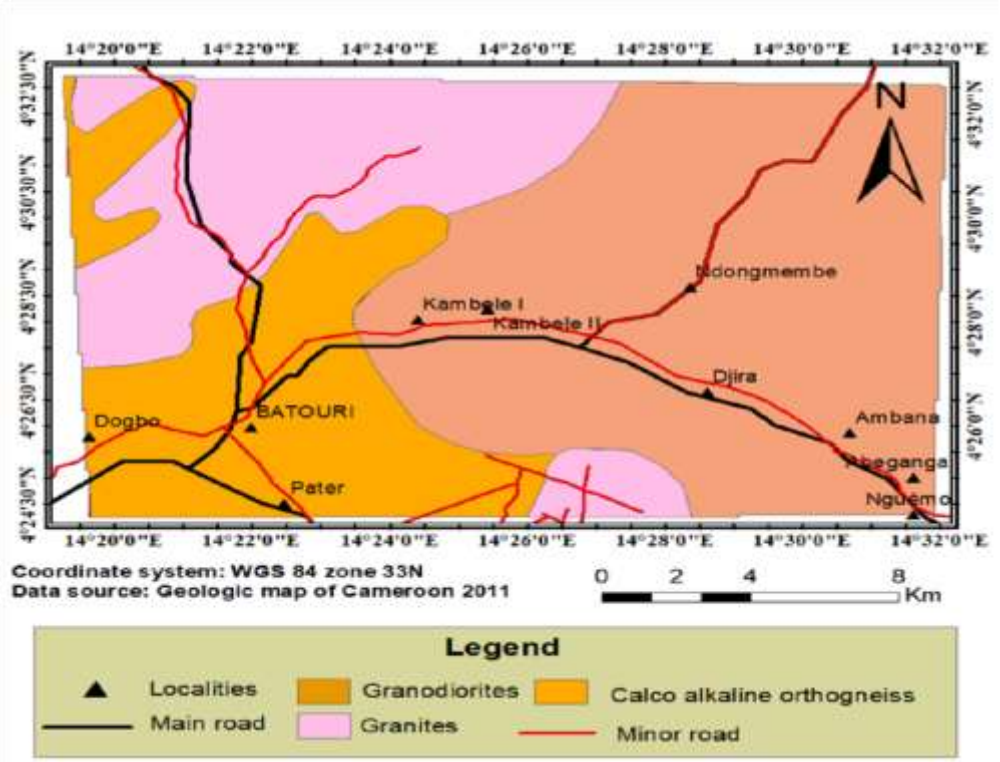

Figure 4: Geologic map of kambele (Geological map of Cameroon, 2011).

ISSN No. 2321-2705 | DOI: 10.51244/IJRSI |Volume XIII Issue VI June 2026

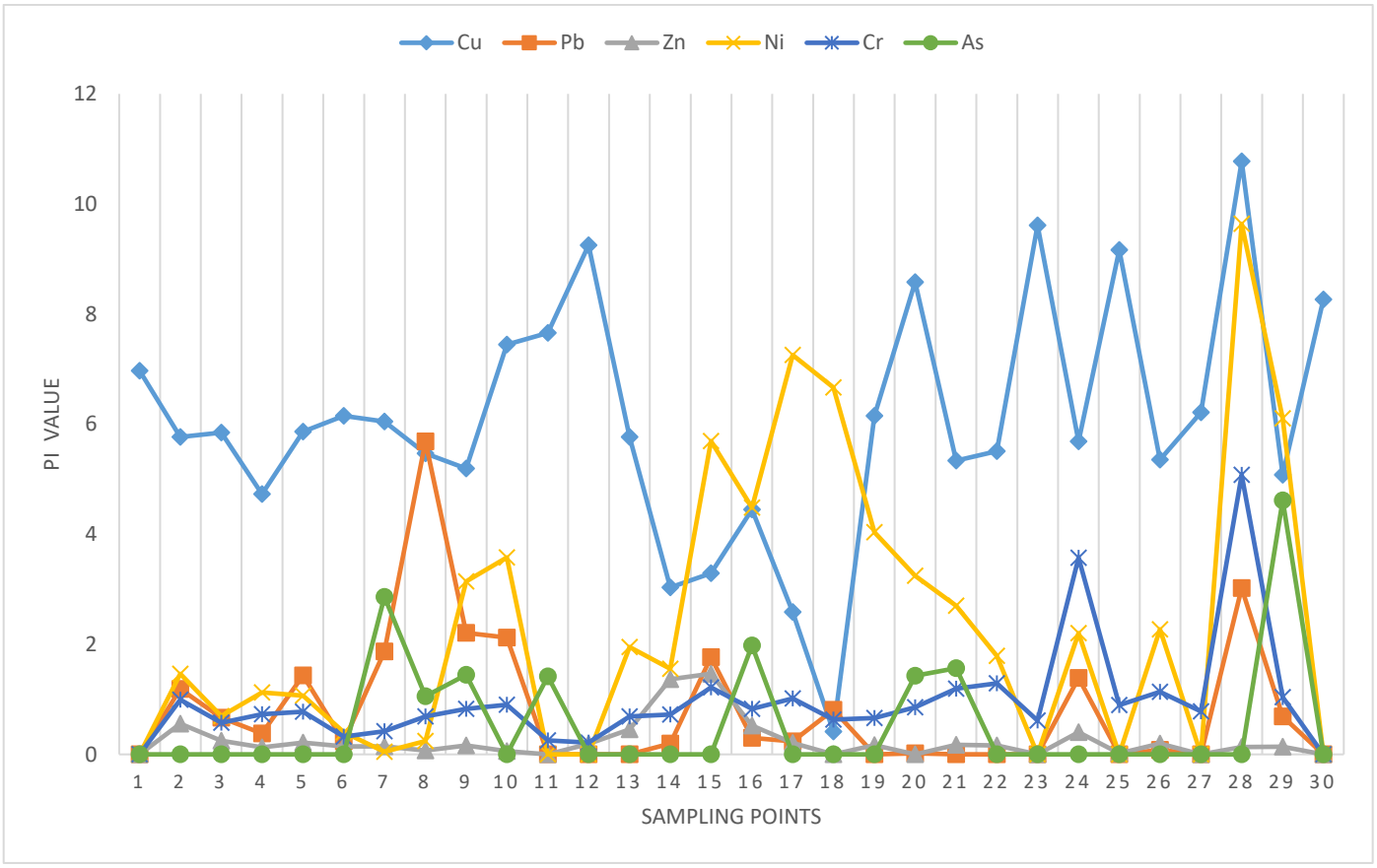

Figure 5: Pollution indices of Samples.

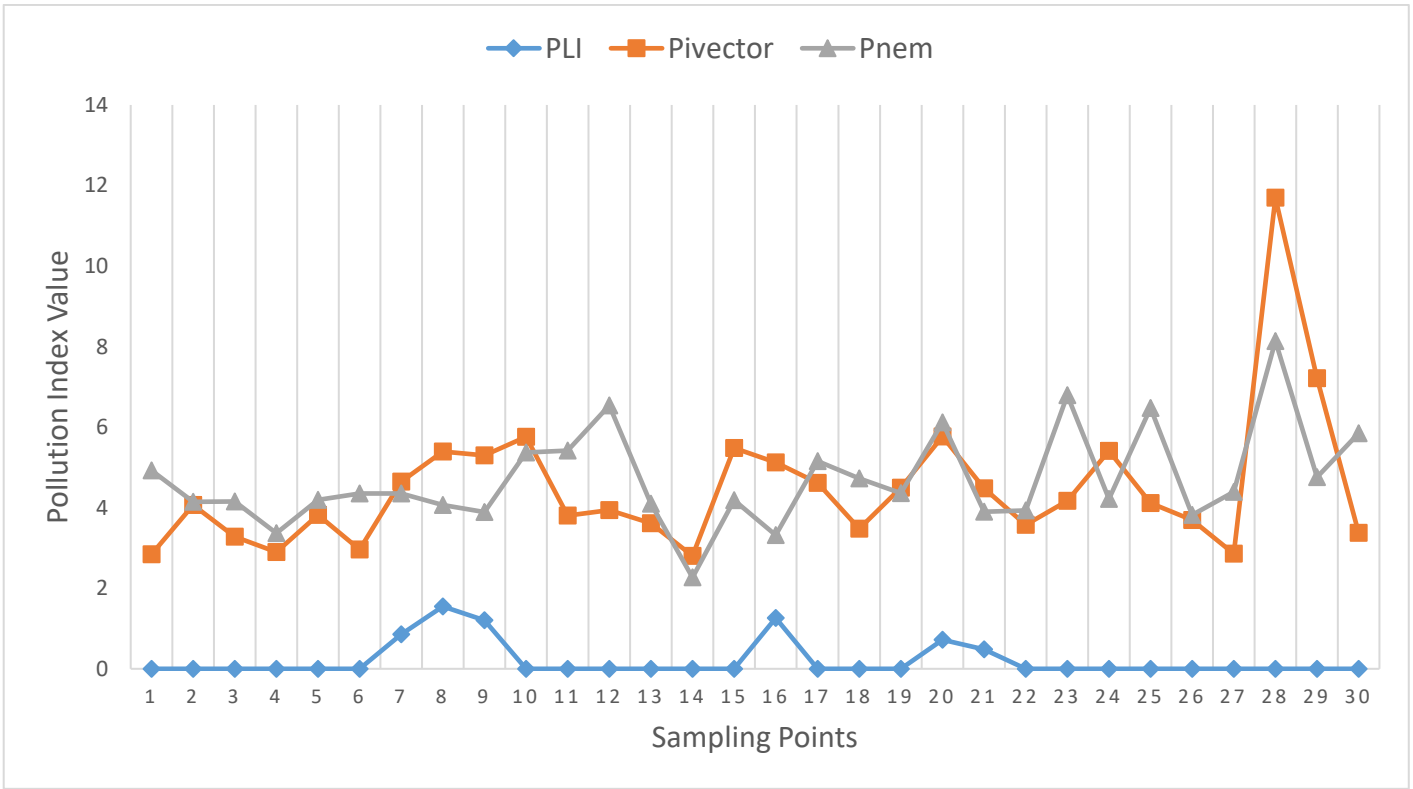

Figure 6: Pollution index, Nemerow pollution index and vector pollution index.

ISSN No. 2321-2705 | DOI: 10.51244/IJRSI |Volume XIII Issue VI June 2026

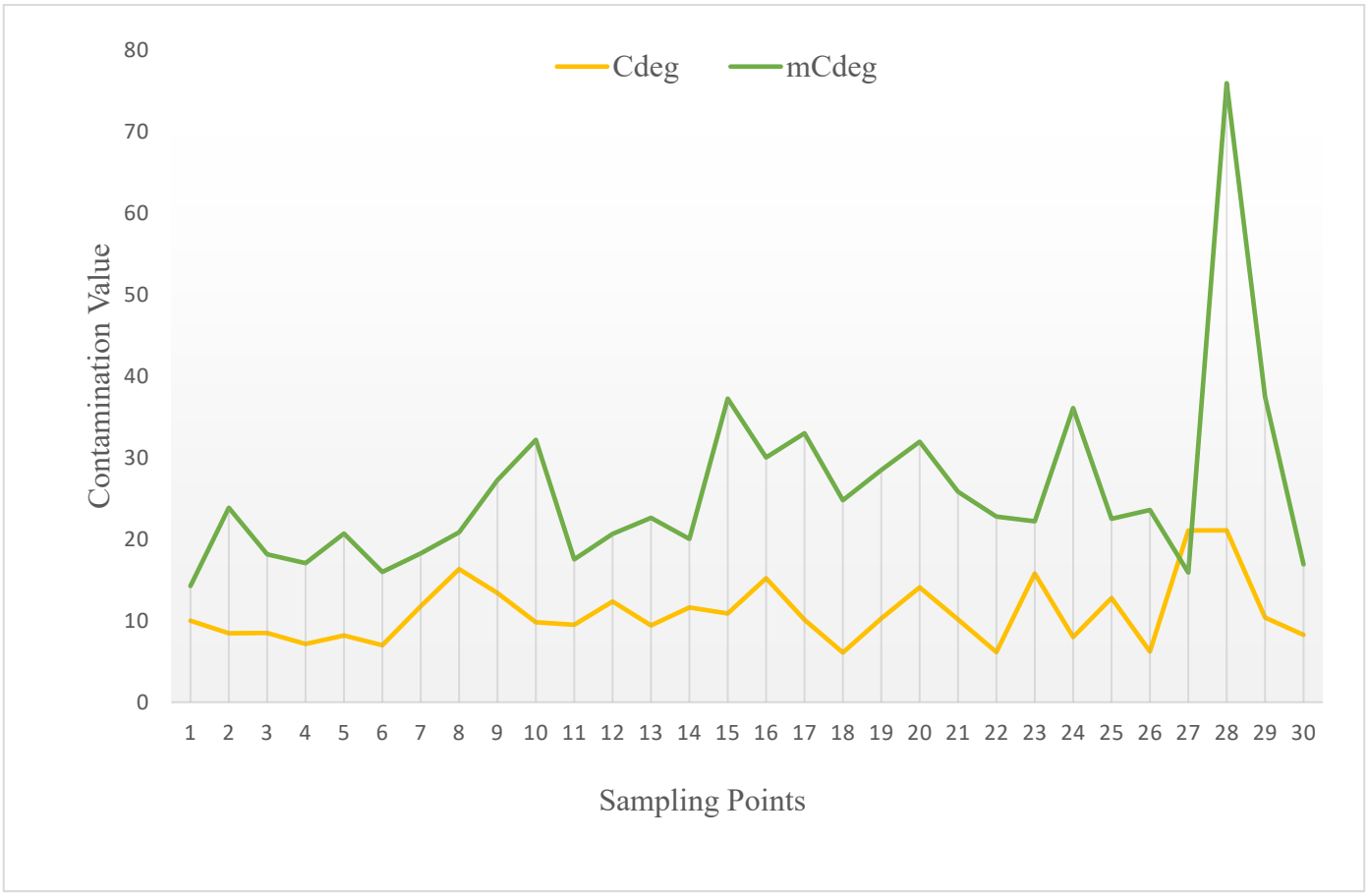

Figure 7: Contamination and modified contamination degree.

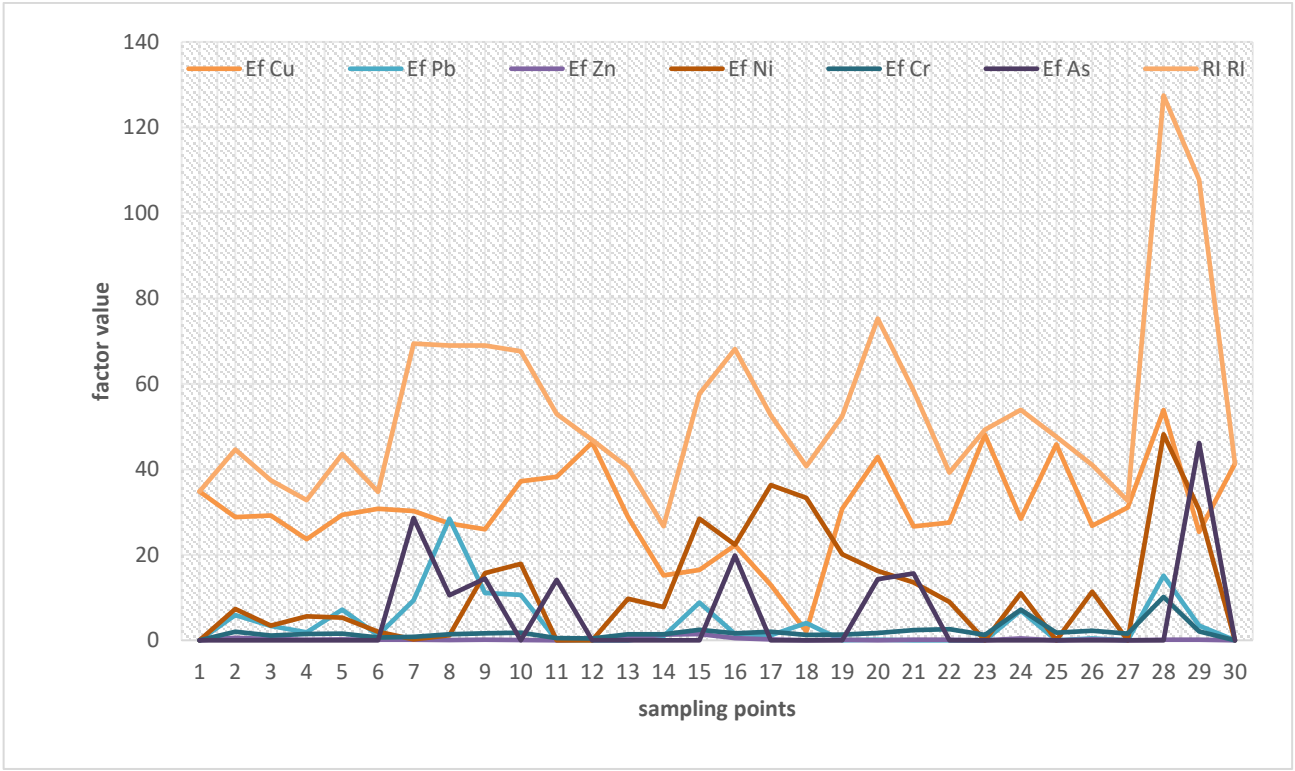

Figure 8: Potential ecological risk

ISSN No. 2321-2705 | DOI: 10.51244/IJRSI |Volume XIII Issue VI June 2026

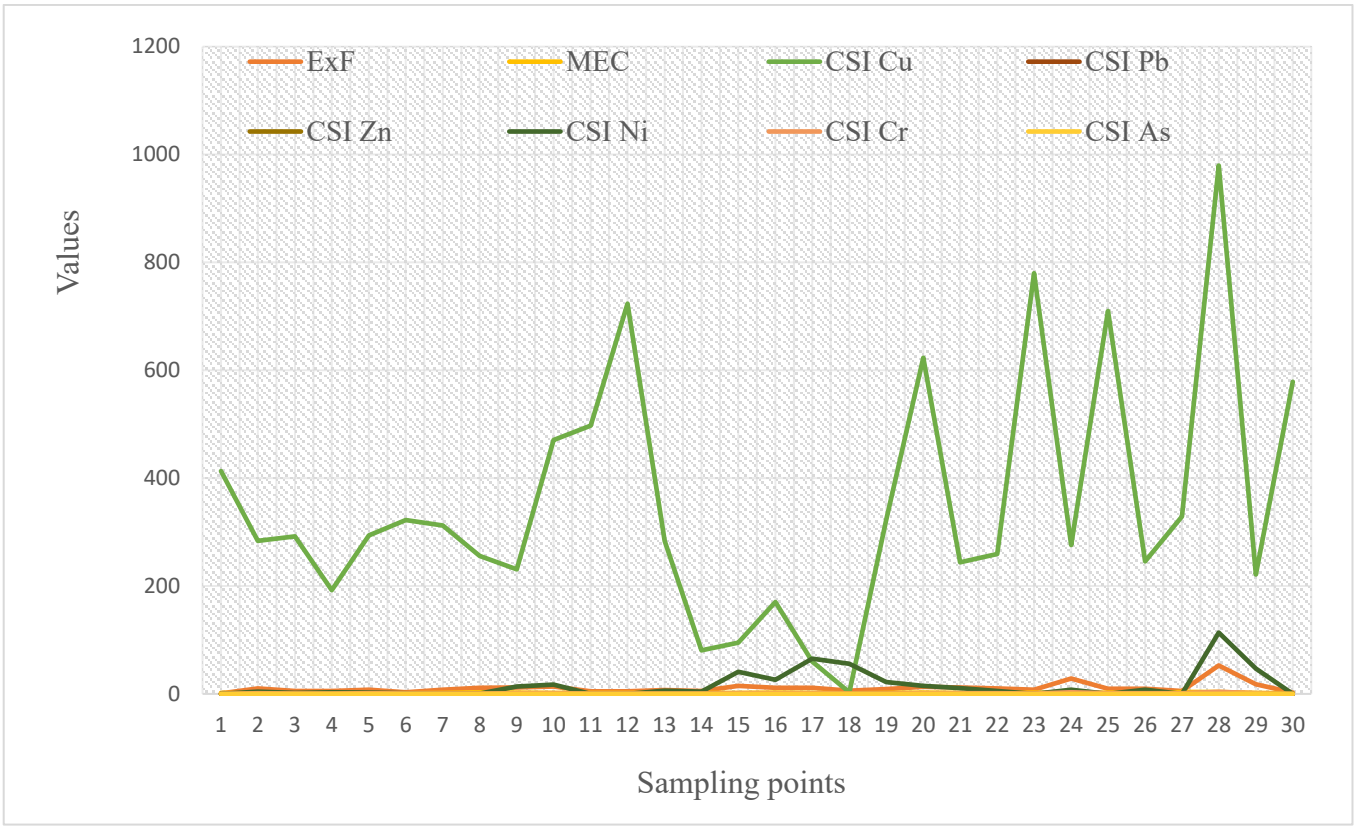

Figure 9: Contamination security index, exposure and multielement contamination factors.

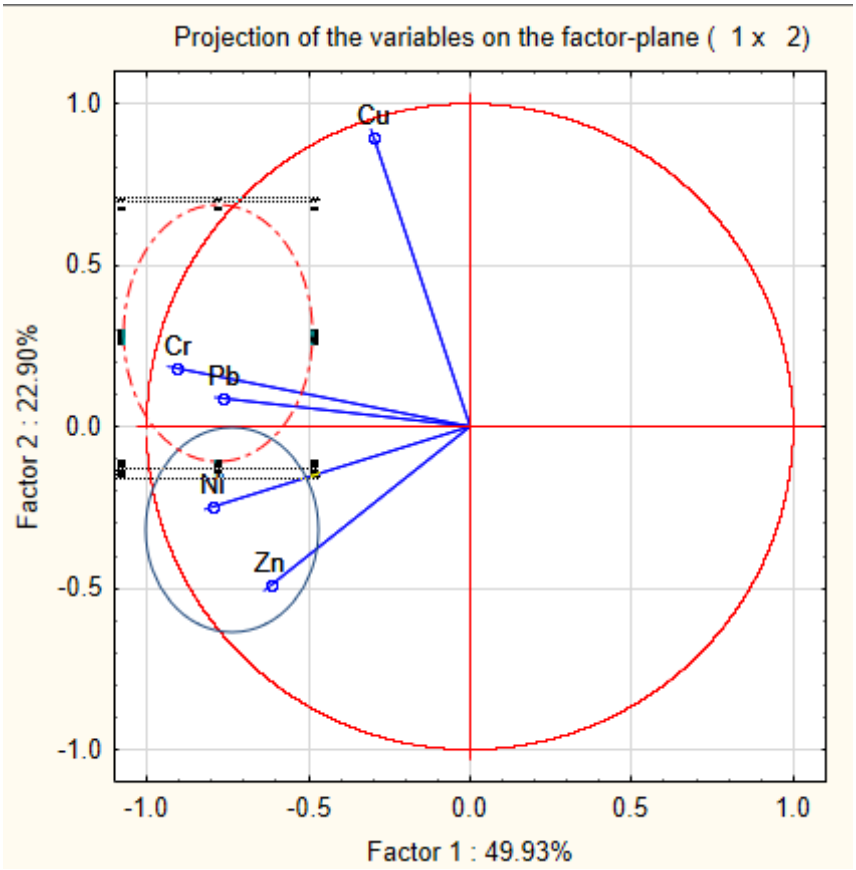

Figure 10: Circle of correlation of PCA on soil chemical parameters

ISSN No. 2321-2705 | DOI: 10.51244/IJRSI |Volume XIII Issue VI June 2026

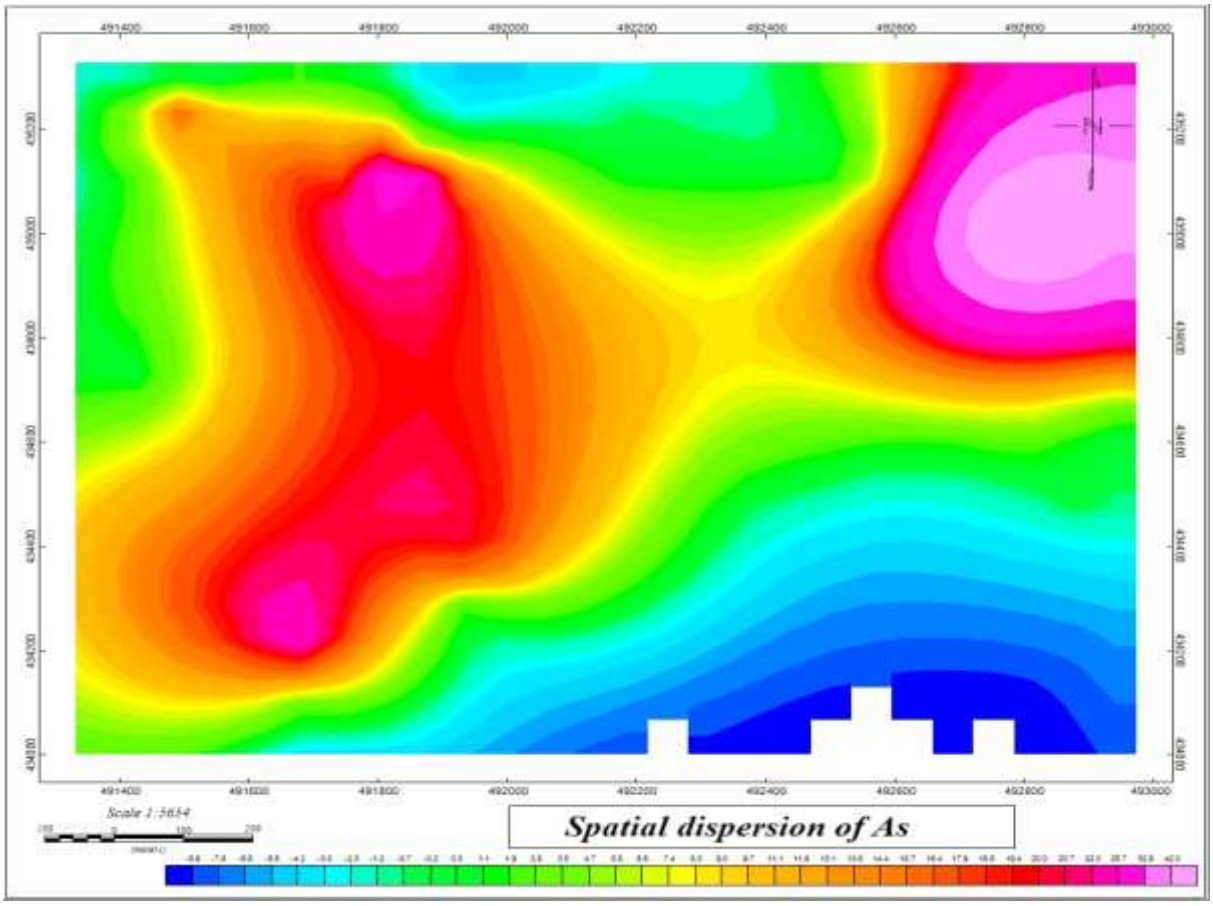

Figure 11: Spatial dispersion of arsenic in Kambele.

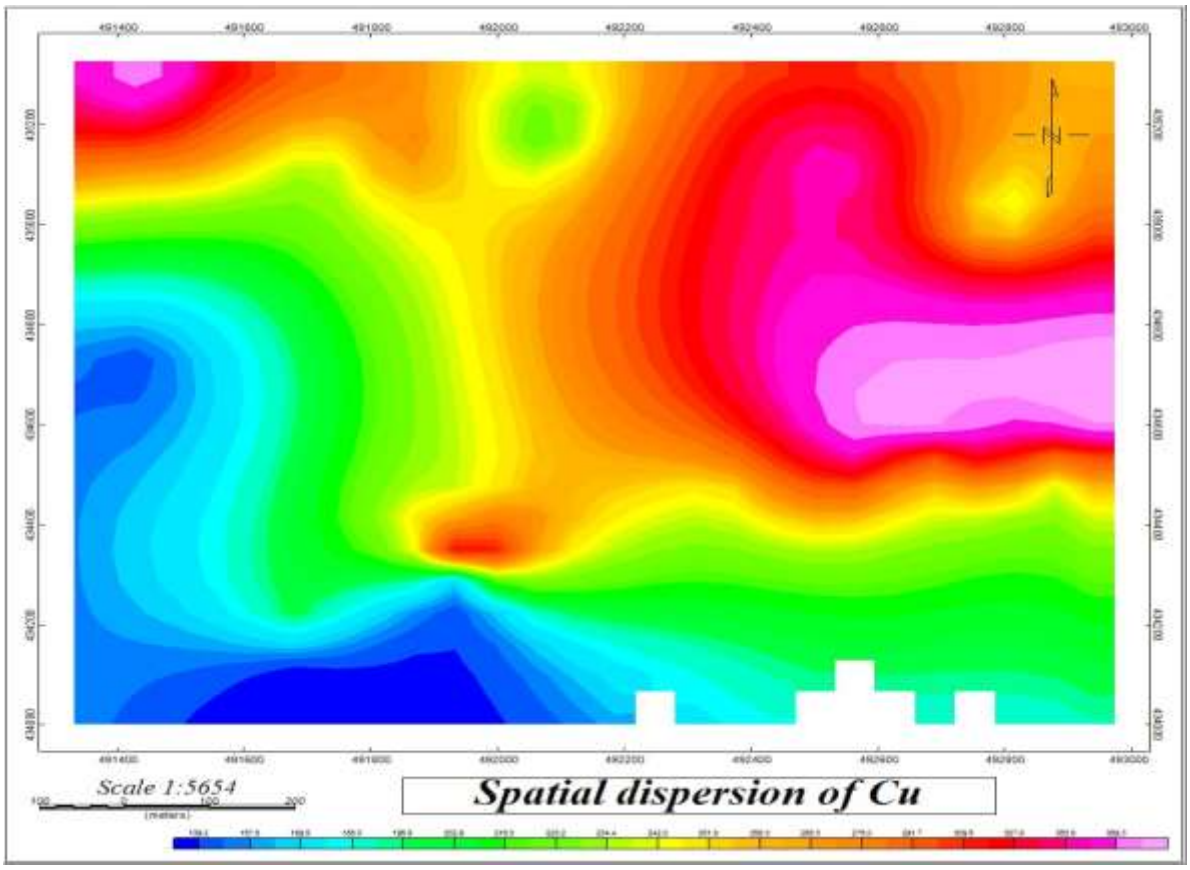

Figure 1: Spatial dispersion of Copper.

ISSN No. 2321-2705 | DOI: 10.51244/IJRSI |Volume XIII Issue VI June 2026

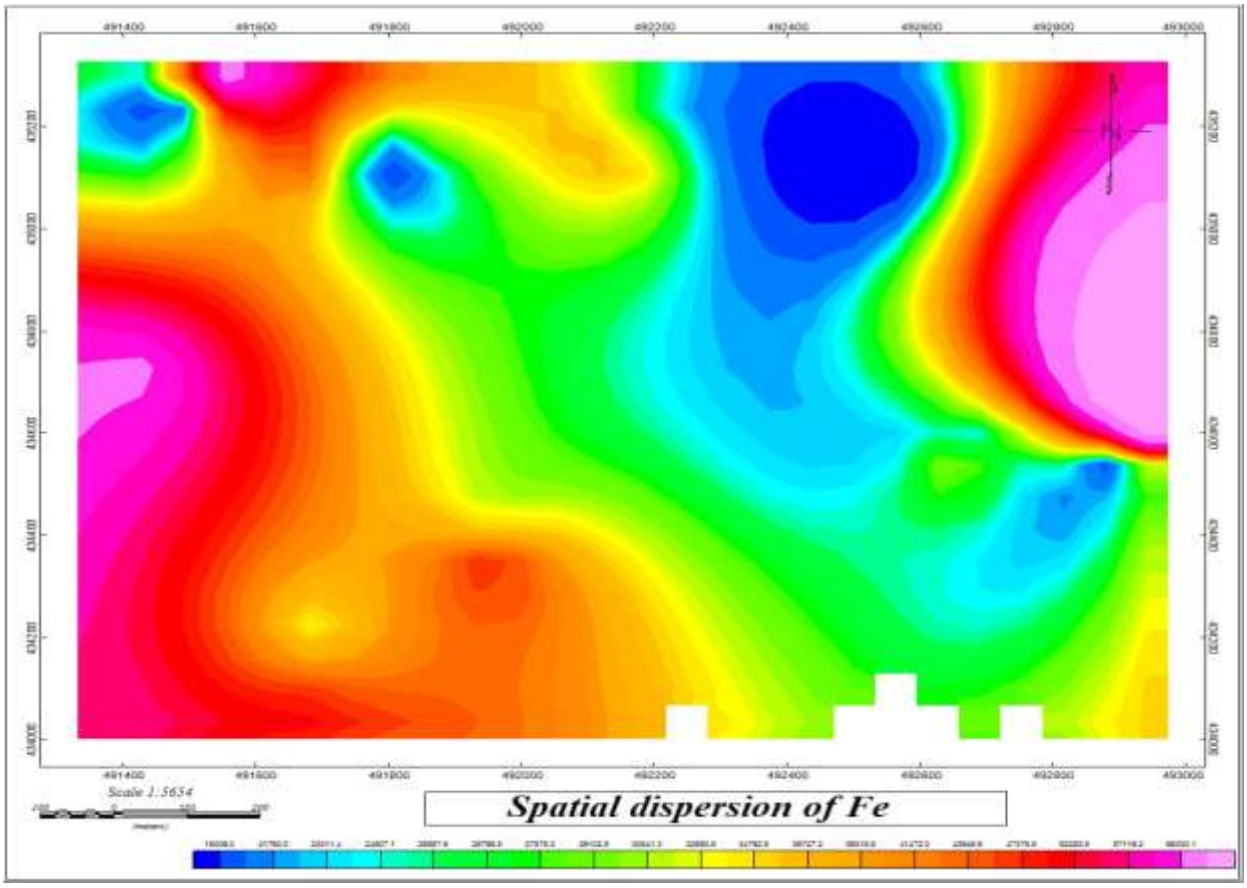

Figure 13: Spatial dispersion of iron

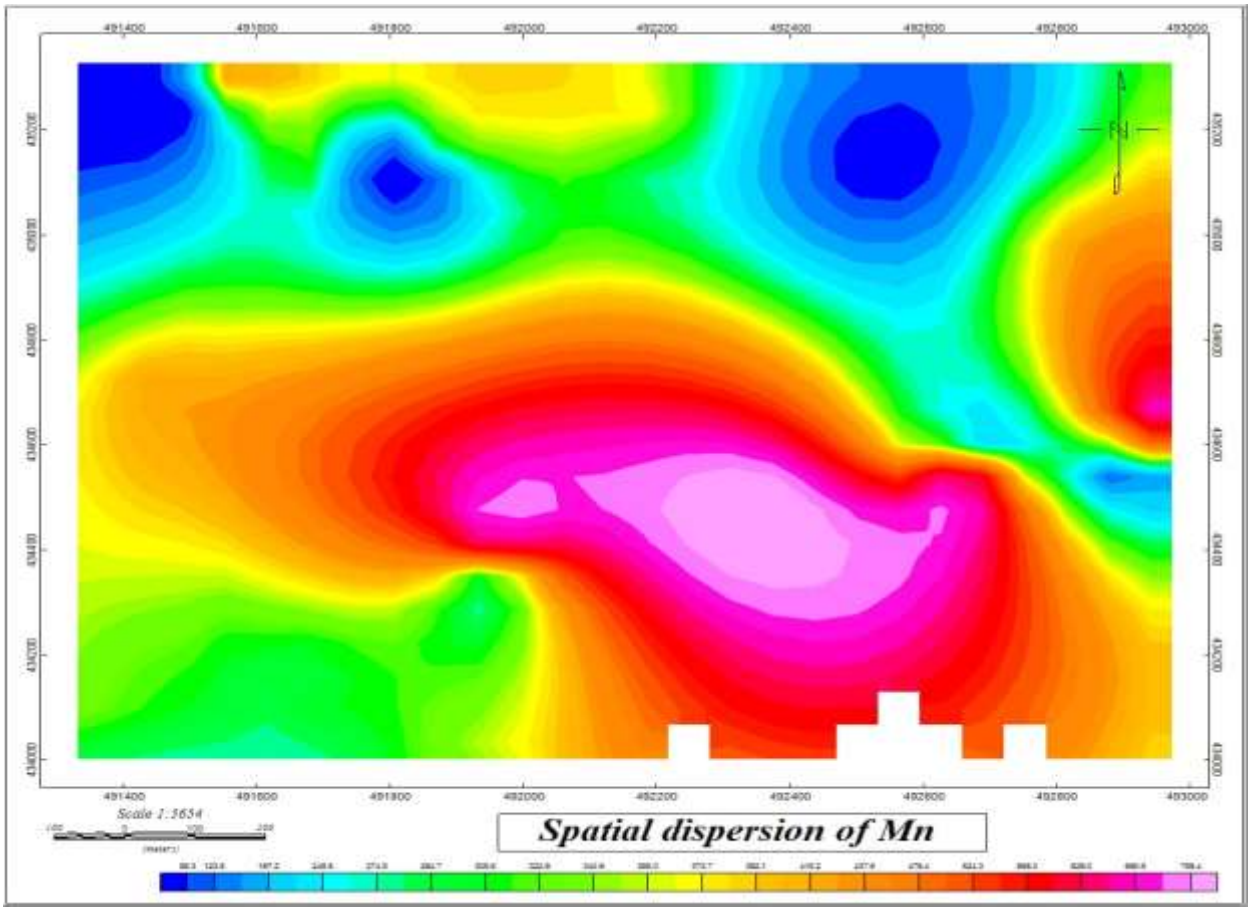

Figure 14: Dispersion of Manganese in Kambele.

ISSN No. 2321-2705 | DOI: 10.51244/IJRSI |Volume XIII Issue VI June 2026

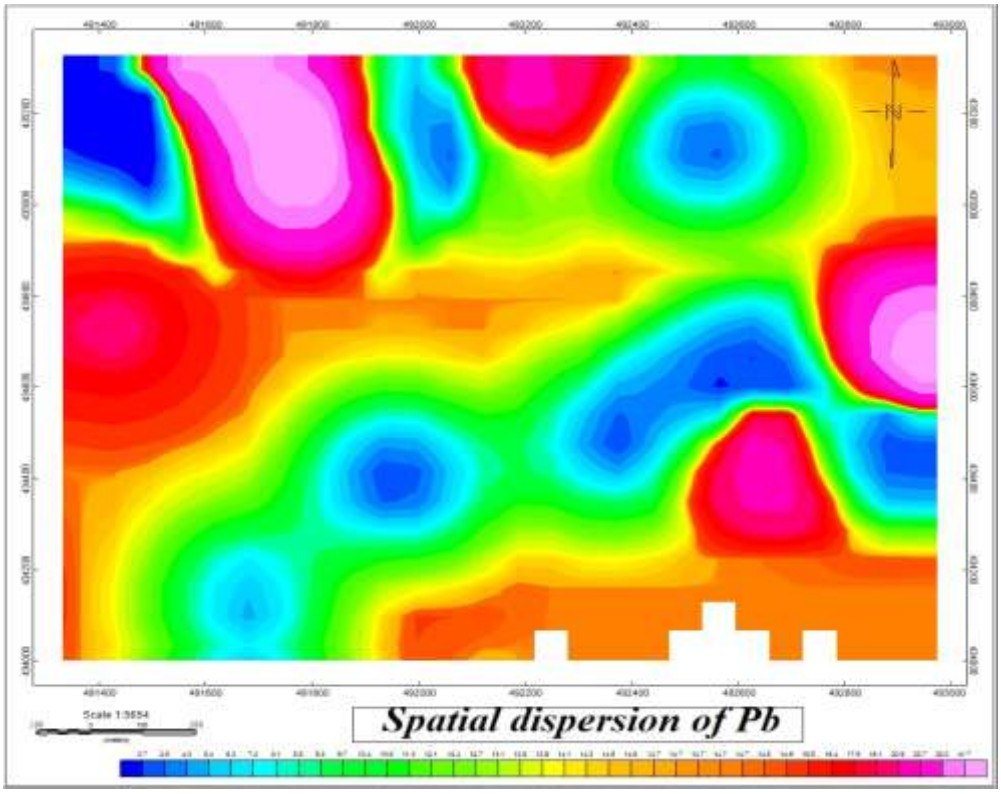

Figure 15: Dispersion of Lead.

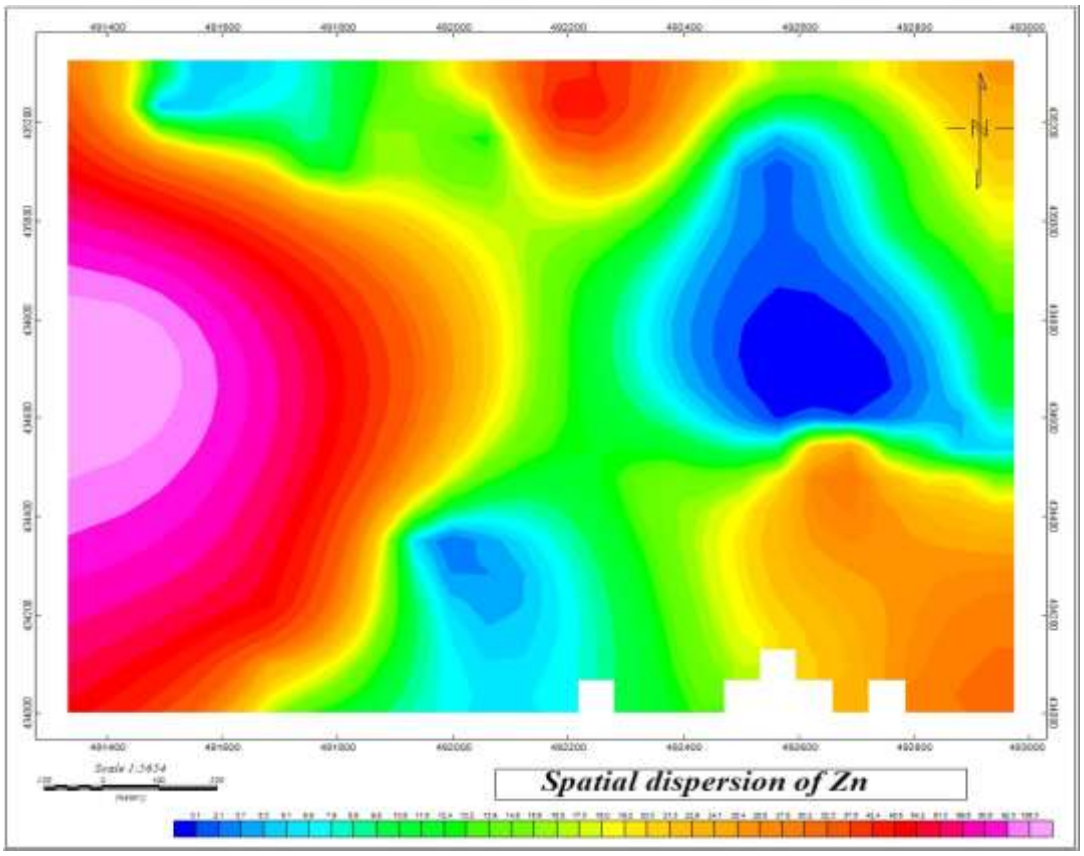

Figure 16: Zinc spatial dispersion.

ISSN No. 2321-2705 | DOI: 10.51244/IJRSI |Volume XIII Issue VI June 2026

TABLE LIST: Table 1: Coordinates of samples collected on June 30, 2021

Sample	Coordinates		Sample	Coordinates		Sample	Coordinates	
E1	4°27'61"	14°25'20"	E11	4°26'47"	14°24'59"	E21	4°27'02"	14°24'32"
E2	4°27'10"	14°24'58"	E12	4°26'46"	14°25'00"	E22	4°27'15"	14°24'34"
E3	4°27'09"	14°24'55'	E13	4°26'44"	14°24'54"	E23	4°27'23"	14°24'37"
E4	4°27'06"	14°24'57"	E14	4°26'44"	14°24'42"	E24	4°27'25"	14°24'36"
E5	4°27'00"	14°24'56"	E15	4°26'45"	14°24'42"	E25	4°27'26"	14°24'37"
E6	4°26'59"	14°24'57"	E16	4°26'53"	14°24'25"	E26	4°27'32"	14°24'34"
E7	4°26'58"	14°24'55"	E17	4°26'53"	14°24'21"	E27	4°27'33"	14°24'36"
E8	4°26'56"	14°24'55	E18	4°27'01"	14°24'28"	E28	4°27'34"	14°24'39"
E9	4°26'54"	14°24'55"	E19	4°27'02"	14°24'27"	E29	4°27'29"	14°24'51"
E10	4°26'48"	14°25'00"	E20	4°27'02"	14°24'30"	E30	4°27'21"	14°24'55"

Table 2: Statistical summary of analysed heavy metals.

	Cr	**Ni**	**Cu**	**Zn**	**Pb**	**Fe**	**Mn**	**As**
mean	87	162	272	23	16	37 292	310	7
median	70	114	261	15	5	31 133	294	0
std	89	175	99	34	25	26 211	249	14
min	0	0	19	0	0	8550	0	0
max	457	655	485	139	114	121 611	885	60
GB	90	68	45	95	20	472	600	13
WHO	100	50	100	50	85	50000	2000	20
CSQG	87	35	63	200	70	nd	nd	nd

nd: not define

ISSN No. 2321-2705 | DOI: 10.51244/IJRSI |Volume XIII Issue VI June 2026

Table 3: comparison of values obtained for the present study with those obtained by other authors

Country	Hg	As	Cd	Pb	Zn	Cu	Ni	Co	Cr	Fe	Mn	Reference
China	0,12±0,09	10,6±6,50	0,24±0,29	39,2± 19,5	112,3±70,6	30±22	28,4± 13,8		59,8±25,6			Sijin et al. (2015)
South Africa	0,09	79,40	0,05	4,79	51,30	42,51	112,06	25,56	278,8			Caspah et al. (2016)
Ghana	1,06±0,65	6,83±2,42	0,19±0,13	19,96±3,11	61,87±16,5	16,03±3,22	41,77±13,60		16,88±2,47	531,5±97	445,6±108	Crentsil et al. (2016)
Sudan				12,46	20,85	19	15,33	5.2		8473	238,1	Mushtaha et al. (2017)
Cameroon		4±2		79±9	40±8	15±7	8±4			39300±200	730±70	Dallou et al. (2018)
Cameroon		70±3		202,96±6	22,6±67	21,5 ±11	37,6±11		90±8			Mominou et al (2018)
Cameroon				22	69	18,5	22,25		152,5	23164,25		Tehna et al. (2019)
Cameroon		5,854		20,667	29,575	44,643	36,441		79,79	383647,5	529,8	Mambou et al. (2020)
Cameroon		7		16	23	272	162		87	37292	310	Present study

Table 4: Physical parameters of soil samples.

	Unit	max	min	mean	std	median	WHO	IASS
MC	%	18,81	1,30	9,49	3,56	9,17	/	/
pH	/	6,22	5,12	5,59	0,25	5,56	6,5-8,5	4-8,5
EC	(µS/cm)	416,00	96,00	213,33	73,44	185,50	1000	40000
OM	%	1,42	0,30	0,70	0,30	0,62	13	>0,86

Table 5: Contamination factors of heavy metals in the site.

	Cu	Pb	Zn	Ni	Cr	As
max	10,8	5,7	1,5	9,6	5,1	4,6
min	0,4	0,0	0,0	0,0	0,0	0,0
median	5,8	0,2	0,2	1,7	0,8	0,0
mean	6,1	0,8	0,2	2,4	1,0	0,5
std	2,2	1,2	0,4	2,6	1,0	1,1

Table 6: Enrichment factor values.

	Cu	Pb	Zn	Ni	Cr	As
min	2	0	0	0	0	0
max	7,40	8,31	1,40	5,98	3.5	0,51
mean	4,71	4,16	0,23	2,99	1,75	0,08
median	0,67	0	0,18	0,18	0,07	0
std	2,70	2,17	0,19	0,12	0,06	0,09

ISSN No. 2321-2705 | DOI: 10.51244/IJRSI |Volume XIII Issue VI June 2026

Table 7: Pollution Indices.

	Cu	Pb	Zn	Ni	Cr	As	PLI	IN	PIvector
max	10,8	5,7	1,5	9,6	5,1	4,6	1,5	8,1	11,7
min	0,4	0,0	0,0	0,0	0,0	0,0	0,0	2,3	2,8
median	5,8	0,2	0,2	1,7	0,8	0,0	0,0	4,4	4,1
mean	6,1	0,8	0,2	2,4	1,0	0,5	0,2	4,7	4,5
std	2,2	1,2	0,4	2,6	1,0	1,1	0,4	1,2	1,7

Table 8: Geoaccumulation index.

	Cu	Pb	Zn	Ni	Cr	As
max	1,2	0,9	0,3	1,1	0,8	0,8
min	-0,3	-2,3	-1,7	-1,2	-0,5	0,0
median	0,9	0,0	-0,6	0,3	0,0	0,0
mean	0,9	-0,1	-0,4	0,3	0,0	0,1
std	0,3	0,6	0,4	0,5	0,3	0,2

Table 9: Contamination Degree.

	Cdeg	mCdeg
max	21,1	75,9
min	6,1	14,3
median	10,1	22,7
mean	11,0	25,8
std	3,9	11,6

Table 10: Potential Ecological Risk.

	Ef						RI
	Cu	Pb	Zn	Ni	Cr	As	
max	53,9	28,4	1,5	48,2	10,2	46,2	127,5

min	2,1	0,0	0,0	0,0	0,0	0,0	26,7
median	29,0	1,2	0,2	8,3	1,6	0,0	48,4
mean	30,3	4,1	0,2	11,9	1,9	5,5	53,8
std	11,0	6,2	0,4	12,9	2,0	10,9	21,8

Table 11: CSI, MEC and ExF.

	ExF	MEC	CSI					
			Cu	Pb	Zn	Ni	Cr	As
Maximum	52,72	3,51	979,58	1,06	0,43	113,65	3,89	0,41
Min	0,97	1,01	2,94	0,00	0,00	0,00	0,00	0,00
Mean	10,71	1,83	351,67	0,25	0,13	15,76	1,04	0,07
Median	9,17	1,69	287,90	0,19	0,13	4,92	0,96	0,00
Std	9,52	0,65	228,23	0,27	0,11	25,62	0,71	0,12

Table 12 : Human Health Risk Assessment Summary

Location	Children HI	Adult HI	Children CR	Adult CR	Risk Classification
E8	2.85	0.92	2.8×10^{-5}	1.2×10^{-5}	High risk
E18	2.31	0.78	2.1×10^{-5}	0.9×10^{-5}	High risk
E28	3.42	1.12	3.6×10^{-5}	1.5×10^{-5}	Very high risk
E29	1.85	0.62	1.8×10^{-5}	0.7×10^{-5}	Moderate risk
Mean	1.24	0.42	1.1×10^{-5}	0.5×10^{-5}	Moderate risk
USEPA Threshold	>1	>1	$>1\times10^{-6}$	$>1\times10^{-6}$	Intervention required

Table 13 : Contamination Severity Classification Zones

Zone	Risk Level	IN Range	RI Range	mCd Range	CSI Range	Recommended Action
I	High	>5.5	>80	>40	>500	Immediate intervention

ISSN No. 2321-2705 | DOI: 10.51244/IJRSI |Volume XIII Issue VI June 2026

II	Medium-high	4.0-5.5	50-80	25-40	200-500	Enhanced monitoring
III	Medium	2.5-4.0	30-50	15-25	50-200	Regular monitoring
IV	Low	<2.5	<30	<15	<50	Baseline monitoring

Supplementary Tables

Table S1 : Certified Reference Material Recoveries (NIST SRM 2710a)

Element	Certified Value (mg/kg)	Measured Value (mg/kg)	Recovery (%)
Cr	34.2 ± 2.0	33.8 ± 1.8	98.8
Ni	17.6 ± 1.2	18.1 ± 1.1	102.8
Cu	120.5 ± 3.0	119.8 ± 2.8	99.4
Zn	695 ± 15	710 ± 18	102.2
Pb	552 ± 8	548 ± 10	99.3
As	155 ± 5	149 ± 6	96.1
Mn	2145 ± 40	2120 ± 45	98.8
Fe (%)	8.5 ± 0.2	8.4 ± 0.2	98.8

Table S2 : Pearson Correlation Matrix for Heavy Metals and Soil Properties

	Cr	Ni	Cu	Zn	Pb	Fe	Mn	As	pH	EC	OM
r	1.00										
i	0.72**	1.00									

ISSN No. 2321-2705 | DOI: 10.51244/IJRSI |Volume XIII Issue VI June 2026

u	0.68**	0.54**	1.00								
n	-0.12	-0.08	-0.15	1.00							
b	0.61**	0.45*	0.49**	0.08	1.00						
e	0.02	-0.11	-0.05	-0.32*	0.08	1.00					
In	0.14	0.08	0.12	-0.28	0.18	0.43*	1.00				
s	0.35*	0.28	0.32	-0.05	0.38*	0.08	0.12	1.00			
H	-0.18	-0.22	-0.15	0.08	-0.05	-0.05	0.02	-0.12	1.00		
C	0.08	0.15	0.12	-0.02	0.18	0.10	0.05	0.22	0.08	1.00	
M	0.25	0.32*	0.28	-0.08	0.22	0.15	0.18	0.24	0.05	0.12	1.00

*Significant at $p < 0.05$; *Significant at $p < 0.01$